

Physics at a Fermilab Proton Driver

April 16, 2005

Executive Summary

In the last few years there has been interest in a new generation of high intensity multi-GeV proton accelerators. At Fermilab, two possible proton driver schemes have been proposed to enable the Main Injector (MI) beam power to be increased by about a factor of five to 2 megawatts. The presently favored scheme is based on a new 8 GeV superconducting (SC) linac that utilizes, and helps develop, Linear Collider technology.

The interest in a new Fermilab Proton Driver is motivated by the exciting discoveries that have been made in the neutrino sector; namely that neutrinos have mass and that neutrinos of one flavor can transform themselves into neutrinos of a different flavor as they propagate over macroscopic distances. This is exciting because it requires new physics beyond the Standard Model. However, we do not yet have a complete knowledge of neutrino masses and mixing. Understanding these neutrino properties is important because neutrinos are the most common matter particles in the universe. In number, they exceed the constituents of ordinary matter (electrons, protons, neutrons) by a factor of ten billion. They probably account for at least as much energy in the universe as all the stars combined and, depending on their exact masses, might also account for a few percent of the so-called “dark matter”. In addition, neutrinos are important in stellar processes. There are 70 billion per second streaming through each square centimeter of the Earth from the Sun. Neutrinos govern the dynamics of supernovae, and hence the production of heavy elements in the universe. Furthermore, if there is CP violation in the neutrino sector, the physics of neutrinos in the early universe might ultimately be responsible for baryogenesis. *If we are to understand “why we are here” and the basic nature of the universe in which we live, we must understand the basic properties of the neutrino.*

To identify the best ways to address the most important open neutrino questions, and to determine an effective, fruitful U.S. role within a global experimental neutrino program, the American Physical Society’s Divisions of Nuclear Physics and Particles and Fields, together with the Divisions of Astrophysics and the Physics of Beams, have recently conducted a “Study on the Physics of Neutrinos”. This study recommended “*... as a high priority, a comprehensive U.S. program to complete our understanding of neutrino mixing, to determine the character of the neutrino mass spectrum, and to search for CP violation among neutrinos*”, and identified, as a key ingredient of the future program, “*A proton driver in the megawatt class or above and neutrino superbeam with an appropriate very large detector capable of observing CP violation and measuring the neutrino mass-squared differences and mixing parameters with high precision.*” The proposed Fermilab Proton Driver would, together with a suitable new detector, fulfill this need by providing a 2 megawatt proton beam at Main Injector (MI) energies for the future “Neutrinos at the Main Injector” (NuMI) program.

The NuMI beam is unique. It is the only neutrino beam that has an appropriate energy and a sufficiently long baseline to produce, due to matter effects, significant changes in the effective oscillation parameters. These matter effects can be exploited to determine the pattern of neutrino masses. Furthermore, when combined with measurements from the much-shorter-baseline T2K experiment being built in Japan, an

appropriate NuMI-based experiment could exploit matter effects to achieve a greatly enhanced sensitivity to CP violation in the neutrino sector.

To obtain sufficient statistical sensitivity to determine the pattern of neutrino masses and search for CP violation over a large region of parameter-space will require a new detector with a fiducial mass of tens of kilotons and a neutrino beam with the highest practical intensity. Hence, the primary motivation for the new Fermilab Proton Driver is to enable an increase in the MI beam power to the maximum that is considered practical. The achievable sensitivity to the pattern of neutrino masses, and to CP violation, will depend on the unknown neutrino mixing angle θ_{13} . Experiments using the NuMI beam in the Fermilab Proton Driver era would be able to search for a finite θ_{13} with a sensitivity well beyond that achievable with the present NuMI beam, the T2K beam, or at future reactor experiments.

In the presently favored 8 GeV SC linac proton driver scheme the MI fill time is very short (<1 ms), which means that the MI can deliver 2 megawatts of beam at any energy from 40 to 120 GeV, and improvements to the MI ramp time can further increase the beam power. The short fill time also means that the majority of the 8 GeV cycles will not be used by the MI. Hence the SC linac could support a second high-intensity physics program using the primary beam at 8 GeV with an initial beam power of 0.5 megawatts, upgradeable to 2 megawatts (a factor of 64 increase of the present 8 GeV Booster beam). Both the primary proton beams (MI and 8 GeV) could be used to create neutrino beams. Both these beams are needed for an extensive program of neutrino scattering measurements. These measurements are not only of interest in their own right, but are also needed to reduce the systematic uncertainties on the neutrino oscillation measurements which arise from our limited knowledge of the relevant neutrino cross sections.

Although neutrino oscillations provide the primary motivation for interest in the Fermilab Proton Driver, the participation in recent proton driver physics workshops has been broader than the neutrino physics community. Note that intense muon, pion, kaon, neutron, and antiproton beams at the Fermilab Proton Driver would offer great flexibility for the future program, and could support a diverse program of experiments of interest to particle physicists, nuclear physicists, and nuclear-astrophysicists. In particular, as the Large Hadron Collider (LHC) and International Linear Collider (ILC) begin to probe the energy frontier, a new round of precision flavor physics experiments would provide information that is complementary to the LHC and ILC data by indirectly probing high mass scales through radiative corrections. This would help to elucidate the nature of any new physics that is discovered at the energy frontier. Examples of specific experiments of this type that could be supported at the Fermilab Proton Driver include (i) at the MI: $K^+ \rightarrow \pi^+ \nu \bar{\nu}$, $K_L \rightarrow \pi^0 \nu \bar{\nu}$, and $K_L \rightarrow \pi^0 e^+ e^-$, and (ii) using the 8 GeV primary beam to produce an intense low energy muon source: muon ($g - 2$) measurements and searches for a muon electric dipole moment, $\mu \rightarrow e\gamma$, and $\mu \rightarrow e$ conversion. Should no new physics be discovered at the LHC and/or ILC then, for the foreseeable future, precision muon, pion, kaon, and neutron measurements at a high-intensity proton source may provide the only practical way to probe physics at higher mass scales.

The main conclusions presented in this report are:

1. Independent of the value of the unknown mixing angle θ_{13} an initial Fermilab Proton Driver long-baseline neutrino experiment will make a critical contribution to the global oscillation program.
2. If θ_{13} is very small the initial Fermilab Proton Driver experiment will provide the most stringent limit on θ_{13} and prepare the way for a neutrino factory. The expected θ_{13} sensitivity exceeds that expected for reactor-based experiments, or any other accelerator-based experiments.
3. If θ_{13} is sufficiently large the initial Fermilab Proton Driver experiment will precisely measure its value, perhaps determine the mass hierarchy, and prepare the way for a sensitive search for CP violation. The value of θ_{13} will guide the further evolution of the Proton Driver neutrino program.
4. The Fermilab Proton Driver neutrino experiments will also make precision measurements of the other oscillation parameters, and conduct an extensive set of neutrino scattering measurements, some of which are important for the oscillation program. Note that the neutrino scattering measurements require the highest achievable intensities at both MI energies and at 8 GeV.
5. The Fermilab Proton Driver could also support a broad range of other experiments of interest to particle physicists, nuclear physicists, and nuclear astrophysicists. These experiments could exploit antiproton- and kaon-beams from the MI, or muon-, pion-, or neutron-beams from the 8 GeV linac. These “low energy” experiments would provide sensitivity to new physics at high mass scales which would be complementary to measurements at the LHC and beyond.

Contents

| | | |
|----------|--|-----------|
| 1 | Introduction | 7 |
| 2 | Neutrino Oscillations | 9 |
| 2.1 | Oscillation Framework and Measurements | 10 |
| 2.2 | The Importance of the Unanswered Questions | 13 |
| 2.2.1 | The importance of θ_{13} | 13 |
| 2.2.2 | The importance of the Mass Hierarchy | 14 |
| 2.2.3 | The importance of CP Violation and δ | 15 |
| 2.2.4 | Other Oscillation Physics | 15 |
| 2.3 | Evolution of the Sensitivity to θ_{13} | 15 |
| 2.3.1 | Conventional Beam Experiments | 17 |
| 2.3.2 | Off-Axis Experiments | 17 |
| 2.3.3 | Reactor Experiments | 18 |
| 2.3.4 | The Evolution | 18 |
| 2.4 | Fermilab Proton Driver Oscillation Physics Program | 21 |
| 3 | Neutrino Scattering | 27 |
| 3.1 | Fundamental Neutrino Properties | 27 |
| 3.1.1 | Cross-Section Measurements for Oscillation Experiments . . . | 28 |
| 3.1.2 | Neutrino-Electron Scattering | 28 |
| 3.2 | Fundamental Properties of Matter | 29 |
| 4 | The Broader Proton Driver Physics Program | 33 |
| 4.1 | Muon Physics | 34 |
| 4.1.1 | The Muon Source | 34 |
| 4.1.2 | Electric Dipole Moment | 36 |
| 4.1.3 | Muon ($g - 2$) | 37 |
| 4.1.4 | Rare Muon Decays | 38 |
| 4.2 | Other Potential Opportunities | 39 |
| 4.2.1 | Kaon Experiments using the MI Beam | 39 |
| 4.2.2 | Pion Experiments using the 8 GeV Beam | 41 |
| 4.2.3 | Neutron Experiments using the 8 GeV Beam | 42 |
| 4.2.4 | Antiproton Experiments using the MI Beam | 43 |
| 5 | Compatibilities and Proton Economics | 45 |
| 6 | Summary | 47 |

1 Introduction

In the last few years there has been interest in a new generation of high intensity multi-GeV proton accelerators capable of delivering a beam of one or a few megawatts. The interest in these high-intensity accelerators is driven by the exciting discoveries that have been made in the neutrino sector; namely that neutrinos have mass and that neutrinos of one flavor can transform themselves into neutrinos of a different flavor as they propagate over macroscopic distances. This requires new physics beyond the Standard Model (SM). To identify the most important open neutrino physics questions, evaluate the physics reach of various proposed ways of answering the questions, and to determine an effective, fruitful U.S. role within a global experimental neutrino program, the American Physical Society’s Divisions of Nuclear Physics and Particles and Fields, together with the Divisions of Astrophysics and the Physics of Beams, have recently conducted a “Study on the Physics of Neutrinos”. The resulting APS report [1] recommended “*... as a high priority, a comprehensive U.S. program to complete our understanding of neutrino mixing, to determine the character of the neutrino mass spectrum, and to search for CP violation among neutrinos.*” The APS study identified, as a key ingredient of the future program, “*A proton driver in the megawatt class or above and neutrino superbeam with an appropriate very large detector capable of observing CP violation and measuring the neutrino mass-squared differences and mixing parameters with high precision.*” A Fermilab Proton Driver would, together with a suitable new detector, fulfill this need by providing a 2 megawatt proton beam at Main Injector (MI) energies for the future “Neutrinos at the MI” (NuMI) program.

Fermilab hosts the U.S. accelerator-based neutrino program and, with the recently completed NuMI beamline, is operating the longest-baseline neutrino beam in the world. The NuMI beam will, for the foreseeable future, provide the only accelerator-based neutrino baseline that is long enough for matter effects to significantly change the effective neutrino oscillation parameters. These matter effects can be exploited to answer one of the key questions in neutrino physics, namely: Which of the two presently viable patterns of neutrino mass is the correct one ? Furthermore, when combined with measurements from the much shorter-baseline T2K experiment being built in Japan, an appropriate NuMI-based experimental program could exploit matter effects and achieve a greatly enhanced sensitivity to CP violation in the neutrino sector.

To obtain sufficient statistical sensitivity to determine the pattern of neutrino masses and search for CP violation over a large region of parameter -space will require a new detector with a fiducial mass of a few tens of kilotons, and a neutrino beam with the highest practical intensity. Hence, the primary motivation for the new Fermilab Proton Driver is to provide an increase in the MI beam power to the maximum that is considered practical, namely 2 megawatts. The achievable sensitivity to the pattern of neutrino masses, and to CP violation, will depend on the unknown neutrino mixing angle θ_{13} . Experiments using the NuMI beam in the Fermilab Proton Driver era would be able to search for a finite θ_{13} with a sensitivity well beyond that achievable with the present NuMI beam, the T2K beam, or at future reactor experiments. For this reason the APS neutrino study report recommended a new proton driver be

constructed as early as is practical. In the illustrative road map given in the APS report, construction begins in 2008, with operation beginning in 2012. In the longer term, should θ_{13} turn out to be close to or beyond the limiting sensitivity of the first round of Fermilab Proton Driver experiments, the Fermilab Proton Driver would offer options for further upgrades to the detector and/or beamline to yield another stepwise improvement in sensitivity. There would also be an option to develop the Fermilab Proton Driver complex to support a neutrino factory.

The preferred Fermilab Proton Driver scheme is based on a new 8 GeV superconducting (SC) linac that utilizes, and helps develop, Linear Collider technology. The MI fill time is very short (< 1 ms), which means that the MI can deliver 2 megawatts of beam at any energy from 40 to 120 GeV, and that improvements to the MI ramp time can further increase the beam power. The short fill time also means that the majority of the 8 GeV cycles will not be used by the MI. Hence the SC linac could support a second high-intensity physics program using the primary beam at 8 GeV with an initial beam power of 0.5 megawatts, upgradeable to 2 megawatts.

Although neutrino oscillations provide the primary motivation for interest in the Fermilab Proton Driver, the community participating in recent proton driver physics workshops has been broader than the neutrino physics community. Note that intense muon, pion, kaon, neutron, and antiproton beams at the Fermilab Proton Driver would offer great flexibility for the future program, and could support a diverse program of experiments of interest to particle physicists, nuclear physicists, and nuclear-astrophysicists. In particular, as the Large Hadron Collider (LHC) and International Linear Collider (ILC) begin to probe the energy frontier, a new round of precision flavor physics experiments would provide information that is complementary to the LHC and ILC data by indirectly probing high mass scales through radiative corrections. This would help to elucidate the nature of any new physics that is discovered at the energy frontier. Examples of specific experiments of this type that could be supported at the Fermilab Proton Driver include (i) at the MI: $K^+ \rightarrow \pi^+ \nu \bar{\nu}$, $K_L \rightarrow \pi^0 \nu \bar{\nu}$, and $K_L \rightarrow \pi^0 e^+ e^-$, and (ii) using the 8 GeV primary beam to produce an intense low energy muon source: muon ($g - 2$) measurements and searches for a muon electric dipole moment, $\mu \rightarrow e\gamma$, and $\mu \rightarrow e$ conversion. Should no new physics be discovered at the LHC and/or ILC then, for the foreseeable future, precision muon, pion, kaon, and neutron measurements at a high-intensity proton source may provide the only practical way to probe physics at higher mass scales.

This document summarizes the physics opportunities that would be provided by a new proton driver at Fermilab. In particular, the physics that could be done with a 2 megawatt MI beam, and the physics that could be done with a 0.5 - 2 megawatt 8 GeV beam. Sections 2 and 3 describe respectively the potential neutrino oscillation and neutrino scattering physics programs. Section 4 describes the broader physics program using muon-, pion-, and neutron-beams produced with a high intensity primary proton beam at 8 GeV, and using kaon- and antiproton-beams produced with the MI primary proton beam. An overview of the complete proton driver program is given in Section 5, and a summary in Section 6.

2 Neutrino Oscillations

Neutrinos are the most common matter particles in the universe. In number, they exceed the constituents of ordinary matter (electrons, protons, neutrons) by a factor of ten billion. They probably account for at least as much energy in the universe as all the stars combined and, depending on their exact masses, might also account for a few percent of the so-called “dark matter”. In addition, neutrinos are important in stellar processes. There are about $7 \times 10^{10} \text{ cm}^{-2} \text{ sec}^{-1}$ streaming through the Earth from the Sun. Neutrinos govern the dynamics of supernovae, and hence the production of heavy elements in the universe. Furthermore, if there is CP violation in the neutrino sector, the physics of neutrinos in the early universe might ultimately be responsible for baryogenesis. *If we are to understand “why we are here” and the basic nature of the universe in which we live, we must understand the basic properties of the neutrino.*

In the last few years solar, atmospheric, and reactor neutrino experiments have revolutionized our understanding of the nature of neutrinos. We now know that neutrinos produced in a given flavor eigenstate can transform themselves into neutrinos of a different flavor as they propagate over macroscopic distances. This means that, like quarks, neutrinos have a non-zero mass, the flavor eigenstates are different from the mass eigenstates, and hence neutrinos mix. However, we have incomplete knowledge of the properties of neutrinos since *we do not know the spectrum of neutrino masses, and we have only partial knowledge of the mixing among the three known neutrino flavor eigenstates.* Furthermore, it is possible that the simplest three-flavor mixing scheme is not the whole story, and that a complete understanding of neutrino properties will require a more complicated framework. In addition to determining the parameters that describe the neutrino sector, the three-flavor mixing framework must also be tested.

The SM cannot accommodate non-zero neutrino mass terms without some modification. We must either introduce right-handed neutrinos (to generate Dirac mass terms) or allow neutrinos to be their own antiparticle (violating lepton number conservation, and allowing Majorana mass terms). Hence *the physics of neutrino masses is physics beyond the Standard Model.* Although we do not know the neutrino mass spectrum, we do know that the masses, and the associated mass-splittings, are tiny compared to the masses of any other fundamental fermion. This suggests that the physics responsible for neutrino mass will include new components radically different from those of the SM. Furthermore, although we do not have complete knowledge of the mixing between different neutrino flavors, we do know that it is qualitatively very different from the corresponding mixing between different quark flavors. The observed difference necessarily constrains our ideas about the underlying relationship between quarks and leptons, and hence models of quark and lepton unification in general, and Grand Unified Theories (GUTs) in particular. Note that in neutrino mass models the seesaw mechanism [2–5] provides a quantitative explanation for the observed small neutrino masses, which arise as a consequence of the existence of right-handed neutral leptons at the GUT-scale. Over the last few years, as our knowledge of the neutrino oscillation parameters has improved, a previous generation of neutrino mass models

has already been ruled out, and a new set of models has emerged specifically designed to accommodate the neutrino parameters. Further improvement in our knowledge of the oscillation parameters will necessarily reject many of these models, and presumably encourage the emergence of new ideas. Hence *neutrino physics is experimentally driven, and the experiments are already directing our ideas about what lies beyond the Standard Model.*

Our desire to understand both the universe in which we live and physics beyond the SM provides a compelling case for an experimental program that can elucidate the neutrino mass spectrum, measure neutrino mixing, and test the three-flavor mixing framework. It seems likely that complete knowledge of the neutrino mass splittings and mixing parameters is accessible to accelerator-based neutrino oscillation experiments. In the following we first introduce the three-flavor mixing framework and identify the critical measurements that need to be made in the future oscillation physics program. The sensitivity of the Fermilab program based on a new Proton Driver is then considered in the context of the global experimental program.

2.1 Oscillation Framework and Measurements

There are three known neutrino flavor eigenstates $\nu_\alpha = (\nu_e, \nu_\mu, \nu_\tau)$. Since transitions have been observed between the flavor eigenstates we now know that neutrinos have non-zero masses, and that there is mixing between the flavor eigenstates. The mass eigenstates $\nu_i = (\nu_1, \nu_2, \nu_3)$ with masses $m_i = (m_1, m_2, m_3)$ are related to the flavor eigenstates by a 3×3 unitary mixing matrix U^ν ,

$$|\nu_\alpha\rangle = \sum_i (U_{\alpha i}^\nu)^* |\nu_i\rangle \quad (1)$$

Four numbers are needed to specify all of the matrix elements, namely three mixing angles ($\theta_{12}, \theta_{23}, \theta_{13}$) and one complex phase (δ). In terms of these parameters

$$U^\nu = \begin{pmatrix} c_{13}c_{12} & c_{13}s_{12} & s_{13}e^{-i\delta} \\ -c_{23}s_{12} - s_{13}s_{23}c_{12}e^{i\delta} & c_{23}c_{12} - s_{13}s_{23}s_{12}e^{i\delta} & c_{13}s_{23} \\ s_{23}s_{12} - s_{13}c_{23}c_{12}e^{i\delta} & -s_{23}c_{12} - s_{13}c_{23}s_{12}e^{i\delta} & c_{13}c_{23} \end{pmatrix} \quad (2)$$

where $c_{jk} \equiv \cos \theta_{jk}$ and $s_{jk} \equiv \sin \theta_{jk}$. Neutrino oscillation measurements have already provided some knowledge of U^ν , which is approximately given by:

$$U^\nu = \begin{pmatrix} 0.8 & 0.5 & ? \\ 0.4 & 0.6 & 0.7 \\ 0.4 & 0.6 & 0.7 \end{pmatrix} \quad (3)$$

We have limited knowledge of the (1,3)-element of the mixing matrix. This matrix element is parametrized by $s_{13}e^{-i\delta}$. We have only an upper limit on θ_{13} and no knowledge of δ . Note that θ_{13} and δ are particularly important because if θ_{13} and $\sin \delta$ are non-zero there will be CP violation in the neutrino sector.

Neutrino oscillations are driven by the splittings between the neutrino mass eigenstates. It is useful to define the differences between the squares of the masses of

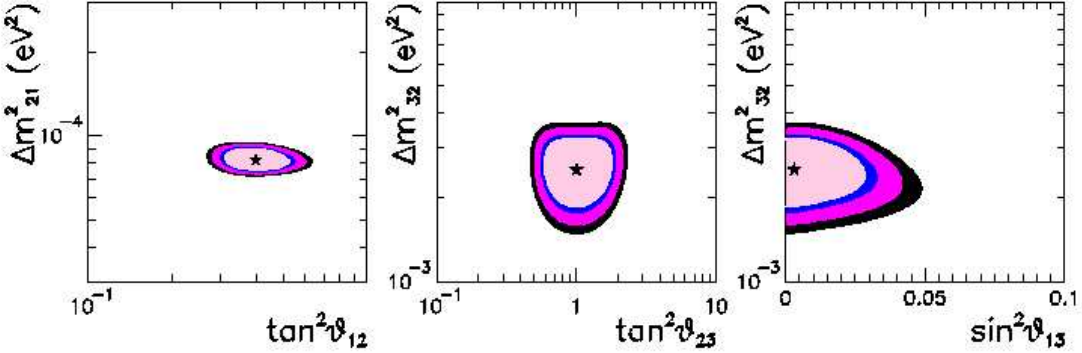


Figure 1: Current experimental constraints on the three mixing angles θ_{12} , θ_{23} , and θ_{13} and their dependence on the two known mass-squared differences Δm_{12}^2 and Δm_{23}^2 . The star indicates the most likely solution. Figure taken from [1].

the mass eigenstates $\Delta m_{ij}^2 \equiv m_i^2 - m_j^2$. The probability that a neutrino of energy E and initial flavor α will “oscillate” into a neutrino of flavor β is given by $P_{\alpha\beta} \equiv P(\nu_\alpha \rightarrow \nu_\beta) = |\langle \nu_\beta | \exp(-i\mathcal{H}t) | \nu_\alpha \rangle|^2$, which in vacuum is given by

$$P_{\alpha\beta} = \left| \sum_{j=1}^3 U_{\alpha j}^* U_{\beta j} \exp(-iE_j t) \right|^2 = \sum_{j=1}^3 \sum_{k=1}^3 U_{\alpha j} U_{\alpha k}^* U_{\beta j}^* U_{\beta k} \exp\left(-i\frac{\Delta m_{kj}^2}{2E} t\right) \quad (4)$$

If neutrinos of energy E travel a distance L then a measure of the propagation time t is given by L/E . Non-zero Δm_{ij}^2 will result in neutrino flavor oscillations that have maxima at given values of L/E , and oscillation amplitudes that are determined by the matrix elements $U_{\alpha i}^\nu$, and hence by θ_{12} , θ_{23} , θ_{13} , and δ .

Our present knowledge of the neutrino mass splittings and mixing matrix, has been obtained from atmospheric [6, 7], solar [8–13], reactor [14–16], and accelerator-based [17] neutrino experiments, and is summarized in Fig. 1. The solar-neutrino experiments and the reactor experiment KamLAND probe values of L/E that are sensitive to Δm_{21}^2 , and the mixing angle θ_{12} . Our knowledge of these parameters is shown in the left panel of Fig. 1. The atmospheric-neutrino experiments and the accelerator based experiment K2K probe values of L/E that are sensitive to Δm_{32}^2 , and the mixing angle θ_{23} . Our knowledge of these parameters is shown in the central panel of Fig. 1. Searches for $\nu_\mu \leftrightarrow \nu_e$ transitions with values of L/E corresponding to the atmospheric-neutrino scale are sensitive to the third mixing angle θ_{13} . To date these searches have not observed this transition, and hence we have only an upper limit on θ_{13} , which comes predominantly from the CHOOZ reactor experiment [14], and is shown in the right panel of Fig. 1.

The mixing angles tell us about the flavor content of the neutrino mass eigenstates. Our knowledge of the Δm_{ij}^2 and the flavor content of the mass eigenstates is summarized in Fig. 2. Note that there are two possible patterns of neutrino mass. This is because the neutrino oscillation experiments to date have been sensitive to the magnitude of Δm_{32}^2 , but not its sign. The neutrino spectrum shown on the left

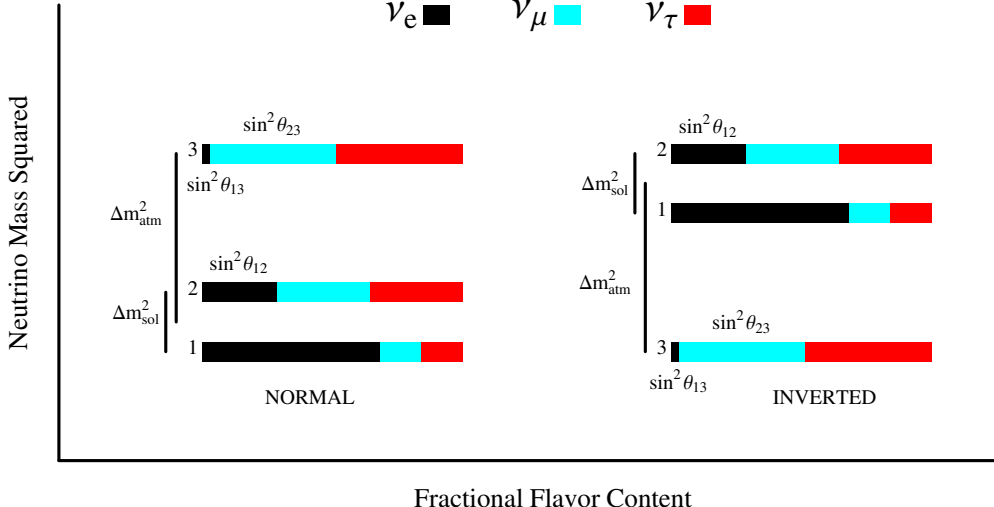


Figure 2: The two possible arrangements of the masses of the three known neutrinos, based on neutrino oscillation measurements. The spectrum on the left corresponds to the *Normal Hierarchy* and has $\Delta m_{32}^2 > 0$. The spectrum on the right corresponds to the *Inverted Hierarchy* and has $\Delta m_{32}^2 < 0$. The ν_e fraction of each mass eigenstate is indicated by the black solid region. The ν_μ and ν_τ fractions are indicated by the blue (red) regions respectively. The ν_e fraction in the mass eigenstate labeled “3” has been set to the CHOOZ bound.

in Fig. 2 is called the *Normal Mass Hierarchy* and corresponds to $\Delta m_{32}^2 > 0$. The neutrino spectrum shown on the right is called the *Inverted Mass Hierarchy* and corresponds to $\Delta m_{32}^2 < 0$. The reason we don’t know the sign of Δm_{32}^2 , and hence the neutrino mass hierarchy, is that neutrino oscillations in vacuum depend only on the magnitude of Δm_{32}^2 . However, in matter the effective parameters describing neutrino transitions involving electron-type neutrinos are modified in a way that is sensitive to the sign of Δm_{32}^2 . An experiment with a sufficiently long baseline in matter and an appropriate L/E can therefore determine the neutrino mass hierarchy.

Finally, it should be noted that there is a possible complication to the simple three-flavor neutrino oscillation picture. The LSND [18] experiment has reported evidence for muon anti-neutrino to electron anti-neutrino transitions for values of L/E which are two orders of magnitude smaller than the corresponding values observed for atmospheric neutrinos. The associated transition probability is very small, of the order of 0.3%. If this result is confirmed by the MiniBooNE [19] experiment, it will require a third characteristic L/E range for neutrino flavor transitions. Since each L/E range implies a different mass-splitting between the participating neutrino mass eigenstates, confirmation of the LSND result would require more than three mass eigenstates. This would be an exciting and radical development. Independent of whether the LSND result is confirmed or not, it is important that the future global neutrino oscillation program is able to make further tests of the three-flavor oscillation framework.

In summary, to complete our knowledge of the neutrino mixing matrix and the

pattern of neutrino masses we must measure θ_{13} and δ , determine the sign of Δm_{32}^2 , and test the three-flavor mixing framework. The primary, initial goal for a Fermilab Proton Driver will be to make these measurements.

2.2 The Importance of the Unanswered Questions

Non-zero neutrino masses require physics beyond the SM. The determination of neutrino masses and mixing will discriminate between various neutrino models (see, for example, Ref. [20–24]) and yield clues that will help determine whether physics beyond the SM is described by a GUT or some other theoretical framework.

The basic neutrino questions that we would like to address with a Fermilab Proton Driver are:

What is the order of magnitude of θ_{13} ?

Is the mass hierarchy normal or inverted?

Is there CP violation in the neutrino sector and what is the value of δ ?

These questions are discussed in the following sections.

2.2.1 The importance of θ_{13}

Neutrino oscillation experiments have shown that two of the neutrino mixing angles (θ_{23} and θ_{12}) are large. This was a surprise since the corresponding mixing angles in the quark mixing matrix are small. We have only an upper limit on the third neutrino mixing angle θ_{13} . From this limit we know that θ_{13} is much smaller than θ_{23} or θ_{12} . However we have no good reason to expect it to be very small. Predictions from recent models are listed in Table 1. Most of the presently viable neutrino mass models predict that θ_{13} is close to the present bound. A value of θ_{13} much smaller than the bound would suggest a new flavor symmetry that suppresses this mixing. However, even if θ_{13} is exactly zero at the GUT scale, radiative corrections would be expected to drive its value away from zero at laboratory energies. If θ_{13} is determined to be much smaller than the present bound we may suspect a new lepton flavor symmetry. If θ_{13} is extremely small, such that $\sin^2 2\theta_{13} \ll 0.001$ for example, its value may place the GUT concept under pressure. In any case *determining the order of magnitude of θ_{13} will discriminate between theoretical models (Table 1) and provide crucial guidance toward an understanding of the physics of neutrino masses.*

In addition to its theoretical importance, the size of θ_{13} has important experimental consequences. If θ_{13} is within an order of magnitude of its present bound we will probably know its value before the “Proton Driver Era”. A Fermilab Proton Driver would then enable the mass hierarchy to be determined and a search for CP violation to be made. If θ_{13} is small ($\sin^2 2\theta_{13} < 0.01$) we will not know its value before the Proton Driver Era. The initial Fermilab Proton Driver program would then improve our knowledge of θ_{13} and prepare the way for a second generation program. If $\sin^2 2\theta_{13} \gtrsim 0.005$ the initial Fermilab Proton Driver experiment would establish

| Model(s) | Refs. | $\sin^2 2\theta_{13}$ |
|---|--|--|
| Minimal SO(10) | [25] | 0.13 |
| Orbifold SO(10) | [26] | 0.04 |
| SO(10) + Flavor symmetry | [27] [28] [29–31] [32–34] | $1.2 \cdot 10^{-6}$ $7.8 \cdot 10^{-4}$ 0.01 .. 0.04 0.09 .. 0.18 |
| SO(10) + Texture | [35] [36] | $4 \cdot 10^{-4}$.. 0.01 0.04 |
| $SU(2)_L \times SU(2)_R \times SU(4)_c$ | [37] | 0.09 |
| Flavor symmetries | [38–40] [41–43] [44–46] [43, 47–50] | 0 $\lesssim 0.004$ 10^{-4} .. 0.02 0.04 .. 0.15 |
| Textures | [51] [52–55] | $4 \cdot 10^{-4}$.. 0.01 0.03 .. 0.15 |
| 3×2 see-saw | [56] [57] (n.h.) (i.h.) | 0.04 0.02 $> 1.6 \cdot 10^{-4}$ |
| Anarchy | [58] | > 0.04 |
| Renormalization group enhancement | [59] | 0.03 .. 0.04 |
| M-Theory model | [23] | 10^{-4} |

Table 1: Selection of predictions for $\sin^2 2\theta_{13}$. The numbers should be considered as order of magnitude statements. The abbreviations “n.h.” and “i.h.” refer to the normal and inverted hierarchies, respectively.

its value and might also determine the mass hierarchy, but would not be sufficiently sensitive to search for CP violation. A second generation program will be required. The options for this second generation include an upgraded detector with or without a new beamline, and a neutrino factory driven by the Proton Driver. Note that *the value of θ_{13} will determine which facilities and experiments will be needed beyond the initial Fermilab Proton Driver experiments to complete the neutrino oscillation program.*

2.2.2 The importance of the Mass Hierarchy

Specific neutrino mass models are usually only compatible with one of the two possible neutrino mass hierarchies (normal or inverted). A measurement of the sign of Δm_{31}^2 would therefore discriminate between models. For example, GUT models with a standard type I see-saw mechanism tend to predict a normal hierarchy (see, for example, the reviews Refs [60, 61]), while an inverted hierarchy is often obtained in models that employ flavor symmetries such as $L_e - L_\mu - L_\tau$ [62, 63].

A determination of the sign of Δm_{31}^2 would also have some consequences for neutrinoless double beta decay experiments. A negative Δm_{31}^2 would imply a lower limit

on the effective mass for neutrinoless double beta decay (in the case of Majorana neutrinos) which would be expected to be within reach of the next generation of experiments.

2.2.3 The importance of CP Violation and δ

Leptogenesis [64], in which CP violation in the leptonic Yukawa couplings ultimately results in a baryon asymmetry in the early Universe, provides an attractive possible explanation for the observed baryon asymmetry. In the most general case, the CP phases involved in leptogenesis are not related to the low-energy CP phases that appear in the effective neutrino mass matrix [65, 66]. However, specific neutrino mass models can yield relationships between the CP violation relevant to leptogenesis and the low-energy CP phases. Indeed, to successfully obtain leptogenesis some models require a non-zero phase δ (see, for example, Refs [56, 67]). Hence, although a measurement of CP violation in the neutrino sector would not establish leptogenesis as the right explanation for the observed baryon asymmetry, it would be suggestive and a measurement of δ would discriminate between explicit neutrino mass models.

2.2.4 Other Oscillation Physics

With a Proton Driver the Fermilab neutrino program would provide a path to the ultimate sensitivity for measurements of θ_{13} , the mass hierarchy, and CP violation. In addition to these crucial measurements, to discriminate between different theoretical models, it will also be important to improve the precision of the other oscillation parameters ($\theta_{12}, \theta_{23}, \Delta m_{21}^2, \Delta m_{32}^2$). Note that θ_{23} is of particular interest as its current, poorly determined, value is consistent with maximal mixing in the (2,3) sector. Is this mixing really maximal? Furthermore the level of consistency between the precisely measured values of the parameters in the various appearance and disappearance modes will test the 3 flavor mixing framework, possibly leading to further exciting discoveries. The Fermilab Proton Driver would not only address the value of θ_{13} , the mass hierarchy, and CP violation, but would also provide a more comprehensive set of measurements that could lead to further unexpected surprises.

2.3 Evolution of the Sensitivity to θ_{13}

In the coming years we can expect improvements in our knowledge of the oscillation parameters from the present generation of running experiments (MiniBooNE, KamLAND, K2K, MINOS, SNO, SuperK) and experiments under construction (T2K). Beyond this a new generation of reactor and accelerator based experiments are being proposed (for example the Double-CHOOZ reactor experiment and the NO ν A experiment using the Fermilab NuMI beam). In the coming decade the search for a non-zero θ_{13} is of particular importance since, not only is θ_{13} the only unmeasured mixing angle, but its value will determine the prospects for determining the mass hierarchy and making a sensitive search for CP violation.

| Label | L | $\langle E_\nu \rangle$ | P_{Source} | Detector technology | m_{Det} | t_{run} |
|---------------------------------------|---------|-------------------------|---------------------------|---------------------|------------------|------------------|
| Conventional beam experiments: | | | | | | |
| MINOS | 735 km | 3 GeV | $3.7 \cdot 10^{20}$ pot/y | Magn. iron calorim. | 5.4 kt | 5 yr |
| ICARUS | 732 km | 17 GeV | $4.5 \cdot 10^{19}$ pot/y | Liquid Argon TPC | 2.35 kt | 5 yr |
| OPERA | 732 km | 17 GeV | $4.5 \cdot 10^{19}$ pot/y | Emul. cloud chamb. | 1.65 kt | 5 yr |
| Off Axis experiments: | | | | | | |
| T2K | 295 km | 0.76 GeV | $1.0 \cdot 10^{21}$ pot/y | Water Cherenkov | 22.5 kt | 5 yr |
| NO ν A [†] | 812 km | 2.22 GeV | $4.0 \cdot 10^{20}$ pot/y | Low-Z-calorimeter | 50 kt | 5 yr |
| Reactor experiments: | | | | | | |
| D-Chooz [†] | 1.05 km | ~ 4 MeV | 2×4.25 GW | Liquid Scintillator | 11.3 t | 3 yr |
| Reactor-II [†] | 1.70 km | ~ 4 MeV | 8 GW | Liquid Scintillator | 200 t | 5 yr |
| † proposed | | | | | | |

Table 2: The different experiments discussed in the text. The table shows, for each experiment, the baseline L , the mean neutrino energy $\langle E_\nu \rangle$, the source power P_{Source} (for beams: in protons on target per year, for reactors: in gigawatts of thermal reactor power), the detector technology, the fiducial detector mass m_{Det} , and the running time t_{run} . Note that most results are, to a first approximation, a function of the product of running time, detector mass, and source power. Table modified from Ref [68].

In this section we describe the expected evolution of our sensitivity to θ_{13} over the next ten to fifteen years, a time period that includes a first generation of Fermilab Proton Driver experiments. A list of relevant experiments and their characteristics is given in Table 2. The $\sin^2 2\theta_{13}$ sensitivities for these experiments are summarized in Fig. 3, where the other oscillation parameters have been chosen to correspond to the present central values. Note that in general the sensitivities of the accelerator based experiments are dominated by statistical uncertainties. To make further progress will require larger detectors and higher intensity beams. Reactor-based experiments, by contrast, are dominated by systematic uncertainties.

In interpreting Fig. 3 it is important to note that it shows the *90% sensitivity* in contrast to the *3σ discovery reach* shown in Figs. 4 and 5. The 90% sensitivity is calculated by setting the “true” value of $\sin^2 2\theta_{13}$ equal to zero in the calculation and then finding the limit on $\sin^2 2\theta_{13}$ that can be set at 90% confidence given all possible values of δ and the mass hierarchy. It is the appropriate quantity to calculate if one wants to understand how low an experiment can set a limit on the value of $\sin^2 2\theta_{13}$. The 3σ discovery reach is calculated by finding the value of $\sin^2 2\theta_{13}$ that can be distinguished from zero at 3σ confidence. It is the appropriate quantity if one is interested in knowing when one can determine that $\sin^2 2\theta_{13}$ is non-zero. Because of the correlated effects of $\sin^2 2\theta_{13}$, δ and the hierarchy (among others) we can determine that $\sin^2 2\theta_{13}$ is non-zero well before measuring its actual value. From the perspective of a Fermilab Proton Driver program the 3σ discovery reach is the more relevant quantity as the interest is in knowing that $\sin^2 2\theta_{13}$ is non-zero. Then one can set about designing an optimised program to go after CP violation and the mass hierarchy.

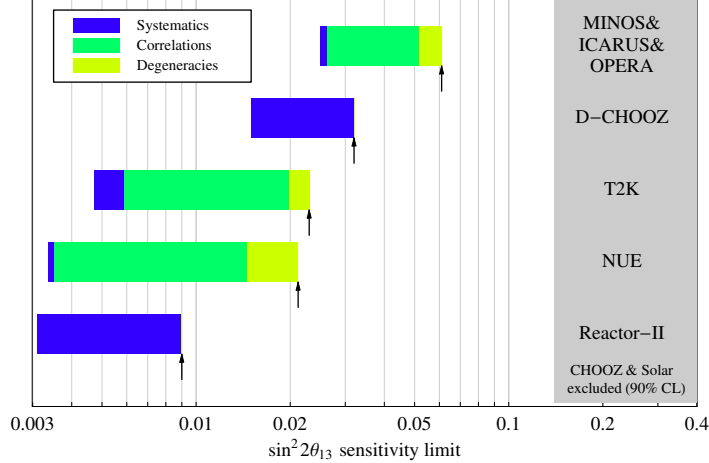


Figure 3: The $\sin^2 2\theta_{13}$ sensitivity limit at the 90% CL for MINOS, ICARUS, and OPERA combined, Double-Chooz, T2K, 2nd generation reactor experiment (Reactor-II), and a NuMI Upgraded Experiment (NUE). Note that for the calculation NUE corresponds to the proposed NO ν A experiment (see Table 2). The left edges of the bars are obtained for the statistics limits only, whereas the right edges are obtained after successively switching on systematics, correlations, and degeneracies, i.e., they correspond to the final $\sin^2 2\theta_{13}$ sensitivity limits. The gray-shaded region corresponds to the current $\sin^2 2\theta_{13}$ bound at 90% CL. For the true values of the oscillation parameters, we use $|\Delta m_{31}^2| = 2.0 \cdot 10^{-3} \text{ eV}^2$, $\sin^2 2\theta_{23} = 1$, $\Delta m_{21}^2 = 7.0 \cdot 10^{-5} \text{ eV}^2$, $\sin^2 2\theta_{12} = 0.8$ [12, 69–71], and a normal mass hierarchy. Figure extended version from Ref. [68].

2.3.1 Conventional Beam Experiments

MINOS is a muon-neutrino disappearance experiment that is expected to confirm the oscillation interpretation of the atmospheric neutrino data and to better determine the associated $|\Delta m^2|$. MINOS will also have some capability to detect electron-neutrino appearance, and hence has some sensitivity to θ_{13} . However, this sensitivity is limited. MINOS is just beginning to take data. In the coming 5 years we expect MINOS to determine θ_{13} if it is very close to the present bound. MINOS is also expected to reduce the uncertainty on $|\Delta m_{31}^2|$ to about $\pm 10\%$.

In Europe, the CNGS program consists of two experiments, ICARUS and OPERA, designed to study tau-neutrino appearance with an L/E corresponding to the atmospheric neutrino oscillation scale. They will also have sensitivity to electron-neutrino appearance, and hence to θ_{13} . The CNGS experiments are expected to begin running in a few years. After 5 years of data taking, the combined sensitivity of ICARUS, OPERA, and MINOS will enable $\sin^2 2\theta_{13}$ to be determined if it exceeds ~ 0.06 .

2.3.2 Off-Axis Experiments

Looking further into the future, significant progress could be made with a new long-baseline experiment that exploits the NuMI beamline, together with a Proton Driver, and a detector that is optimized to detect ν_e appearance. In the following we will refer to this generic NuMI Upgraded Experiment as NUE. There are several possible detector technology choices for NUE. There are also choices for the central beam energy and baseline, which are related to choices about whether the detector is on-axis

(with respect to the central beam direction) or off-axis. In the following we have exploited the calculations available from the NO ν A collaboration to obtain a quantitative understanding of the achievable sensitivity at a 2 megawatt Proton Driver. Hence, NUE numbers and figures in the following discussion correspond to a 50 kt detector placed about 15 mrad off-axis from the NuMI beamline, and a baseline of 812 km. Although no NuMI upgraded experiment has yet received final approval, we might imagine that NO ν A, or an equivalent experiment, is approved, constructed, and becomes operational in 5-10 years from now. Based on NO ν A calculations, after 5 years of data taking we would expect NUE to determine $\sin^2 2\theta_{13}$ if it exceeds ~ 0.02 .

In Japan the JPARC beamline for T2K, a high-statistics, off-axis, second generation version of K2K, has been approved, and is expected to be completed in 2009. With 5 years of data taking T2K is expected to determine $\sin^2 2\theta_{13}$ if it exceeds ~ 0.02 . The combined NUE and T2K sensitivity would be in the range 0.01-0.02.

2.3.3 Reactor Experiments

A new generation of reactor experiments are being proposed with detectors and baselines chosen to be sensitive to θ_{13} . Although choices still have to be made to determine which of these experiments are supported, it seems reasonable to assume that one or two reactor experiments will be executed in the coming decade. The Double-CHOOZ experiment appears to be furthest along in the approval process. This experiment is expected to determine $\sin^2 2\theta_{13}$ if it exceeds ~ 0.03 . Beyond this, a more ambitious reactor experiment, referred to in Table 2 as Reactor II, might be expected to reach a sensitivity $\sin^2 2\theta_{13}$ approaching 0.01 at 90% confidence (the curves in Figs. 4 and 5 are for 3σ discovery). This sensitivity is limited by systematic uncertainties but, if achieved, will be slightly better, for some values of δ , than the corresponding sensitivity expected for T2K, but worse for other values of δ .

2.3.4 The Evolution

The anticipated evolution of the $\sin^2 2\theta_{13}$ discovery reach of the global neutrino oscillation program is illustrated in Fig. 4. The sensitivity is expected to improve by about an order of magnitude over the next decade. This progress is expected to be accomplished in several steps, each yielding a factor of a few increased sensitivity. During this first decade the Fermilab program will have contributed to the improving global sensitivity with MINOS, followed by NUE. MINOS is the on-ramp for the US long-baseline neutrino oscillation program. NUE would be the next step. Note that we assume that NUE starts taking data with the existing beamline before the Proton Driver era. The Proton Driver would take NUE into the fast lane of the global program. Also note that the accelerator based and reactor based experiments are complementary. In particular, the reactor experiments make disappearance measurements, limited by systematic uncertainties. The NUE experiment is an appearance experiment, limited by statistical uncertainties, and probes regions of parameter space beyond the reach of the proposed reactor experiments.

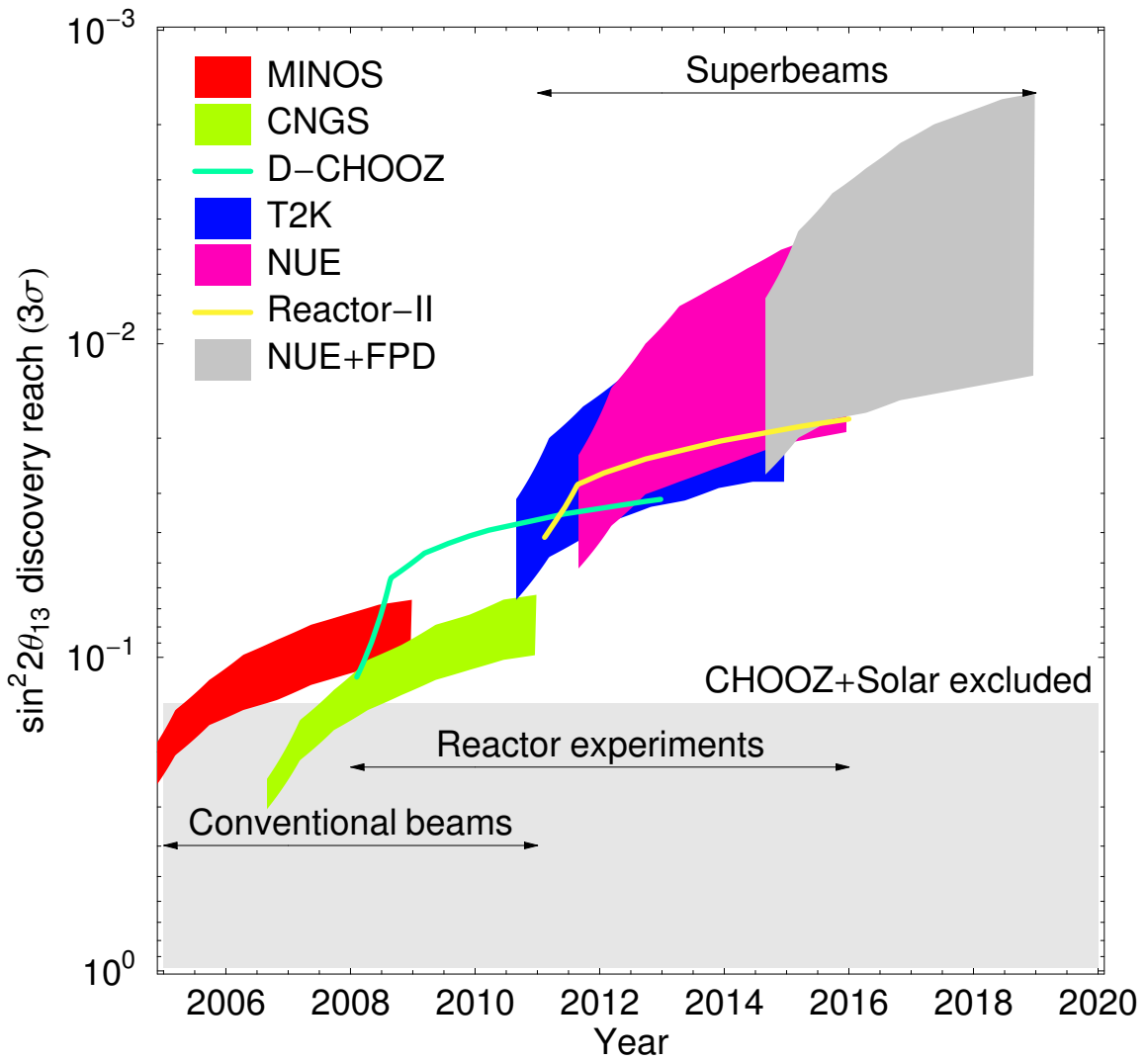


Figure 4: Anticipated evolution of the $\sin^2 2\theta_{13}$ discovery reach for the global neutrino program. The curves show the 3σ sensitivities for each experiment to observe a non-zero value of $\sin^2 2\theta_{13}$. The bands reflect the dependence of the sensitivity on the CP violating phase δ . The calculations are based on the experiment simulations in Refs. [68, 72] and include statistical and systematic uncertainties and parameter correlations. They assume a normal hierarchy and $\Delta m_{31}^2 = 2.5 \cdot 10^{-3} \text{ eV}^2$, $\sin^2 2\theta_{23} = 1$, $\Delta m_{21}^2 = 8.2 \cdot 10^{-5} \text{ eV}^2$, $\sin^2 2\theta_{12} = 0.83$. All experiments are operated with neutrino running only and the full detector mass is assumed to be available right from the beginning. The starting times of the experiments have been chosen as close as possible to those stated in the respective LOIs. The NUE numbers correspond to NO ν A. Reactor-II and FPD refer, respectively, to a 2nd generation reactor experiment and to the Fermilab Proton Driver.

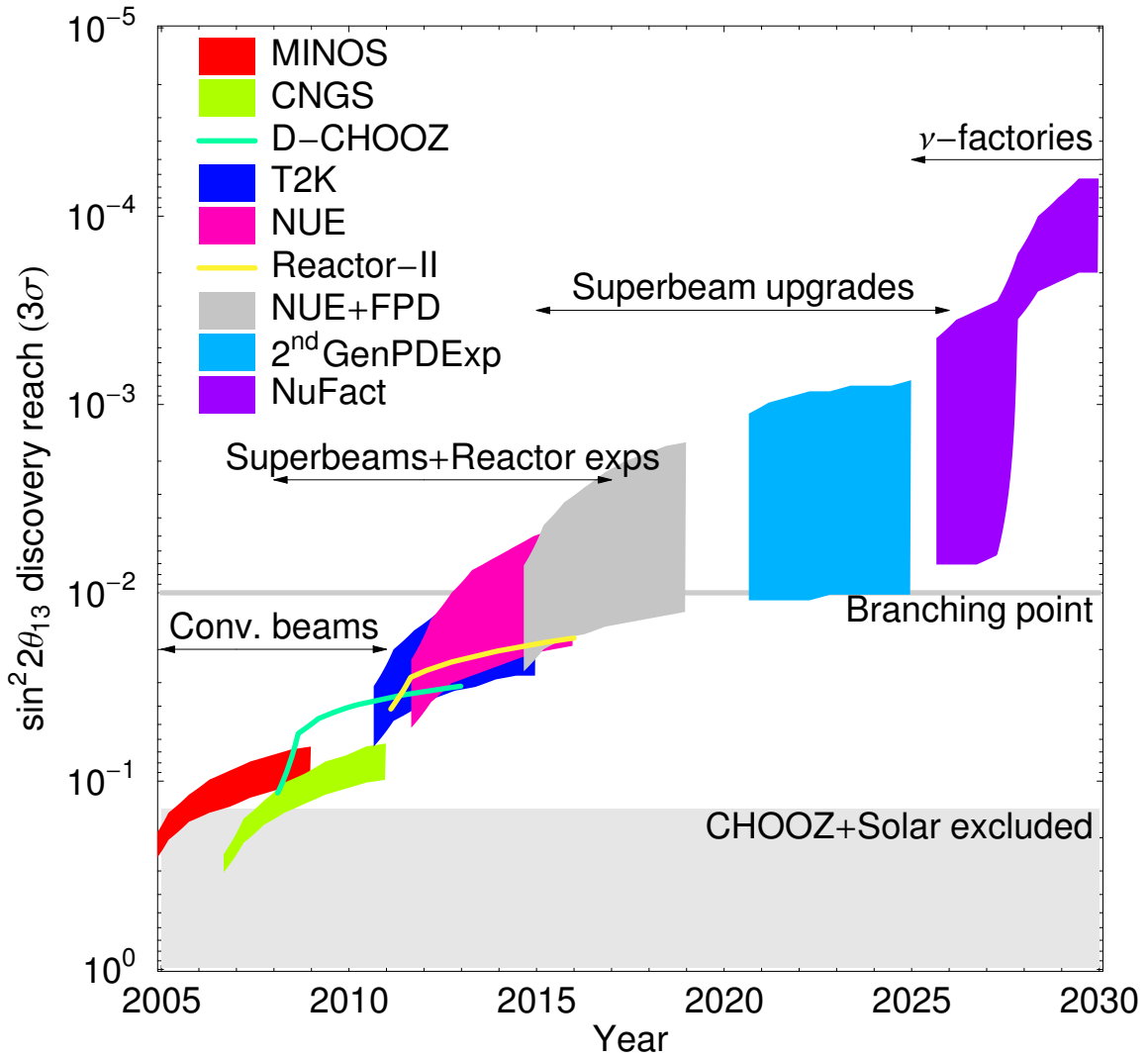


Figure 5: Anticipated evolution of the $\sin^2 2\theta_{13}$ discovery reach for the global neutrino program. See caption for Fig. 4 for details. The “branching point” refers to the decision point for the experimental program (rather than the Fermilab Proton Driver), i.e., between an upgraded beam and/or detector and a neutrino factory program. The upgrade 2ndGenPDEExp (Second Generation Proton Driver Experiment) is assumed to start ten years after T2K starts and the curve uses numbers from the T2HK proposal. The neutrino factory is assumed to start about ten years after the branching point and to switch polarity after 2.5 years.

2.4 Fermilab Proton Driver Oscillation Physics Program

Independent of the value of θ_{13} the initial Fermilab Proton Driver long-baseline neutrino experiment (NUE+FPD) is expected to make an important contribution to the global oscillation program. If θ_{13} is very small NUE+FPD would be expected to provide the most stringent limit on this important parameter, and prepare the way for a neutrino factory. If θ_{13} is sufficiently large, NUE+FPD would be expected to measure its value, perhaps determine the mass hierarchy, and prepare the way for a sensitive search for CP violation. The evolution of the Fermilab Proton Driver physics program beyond the initial experiments will depend not only on θ_{13} , but also on what other neutrino experiments will be built elsewhere in the world. In considering the long-term evolution of the Fermilab Proton Driver program we must take into account the uncertainty on the magnitude of θ_{13} and consider how the global program might evolve.

We begin by considering the evolution of the program if $\sin^2 2\theta_{13} < 0.01$. In this case we will know that ultimately we will need a neutrino factory to complete all of the important oscillation measurements. The initial Fermilab Proton Driver experiment would be a search experiment that would improve the limit on, or establish the value of, θ_{13} . Fig. 5 shows a longer-term version of the $\sin^2 2\theta_{13}$ discovery reach versus time plots shown in Fig. 4. The initial Fermilab Proton Driver experiment would begin to explore the region below $\sin^2 2\theta_{13} \sim 0.01$ and could be upgraded to further improve the sensitivity by a factor of a few. The neutrino factory would ultimately provide a two orders of magnitude improvement in sensitivity.

We have no reason to expect a very small value for θ_{13} . Hence, as the global program achieves increasing sensitivity to θ_{13} , at any time a finite value might be established, and the focus of the program will change from searching for evidence for $\nu_\mu \leftrightarrow \nu_e$ transitions to measuring θ_{13} , determining the mass hierarchy, and searching for CP violation. To explore how in this case the Fermilab Proton Driver would contribute to the global program we consider four cases:

Case 1: No Fermilab Proton Driver and no upgrade to the T2K beam.

Case 2: An upgrade to the T2K beam, but no Fermilab Proton Driver.

Case 3: A Fermilab Proton Driver, but no upgrade to the T2K beam.

Case 4: Both a Fermilab Proton Driver and an upgraded T2K beam.

The prospects for determining the neutrino mass hierarchy and discovering CP violation depend upon the values of θ_{13} and δ . Figures 6, 7, 8 and 9 show as a function of $\sin^2 2\theta_{13}$, for various combinations of experiments, the fraction of all possible values of δ for which the mass hierarchy can be determined (left panels) and CP violation can be discovered (right panels).

The first case, where there is no Fermilab Proton Driver and no upgrade to the T2K beam, is shown in Fig. 6. Note that even by combining T2K and NUE data, one cannot arrive at a 3σ determination for CP violation. If, in addition to no Fermilab Proton Driver, there is no NUE then T2K alone will not be able to determine the

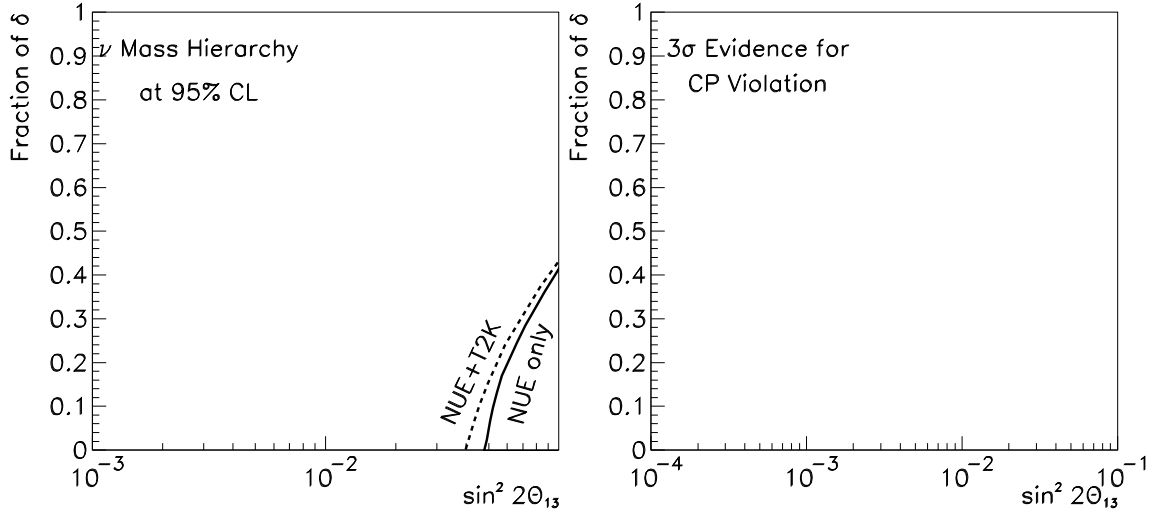


Figure 6: **Case 1: No Fermilab Proton Driver and no upgrade to the T2K beam.** Regions of parameter space where the mass hierarchy (left) and CP violation (right) can be observed at 95% CL and at 3σ , respectively. Note that CP violation would not be visible at all and T2K alone is not sensitive to the hierarchy. NUE, T2K, etc are defined in Table 3.

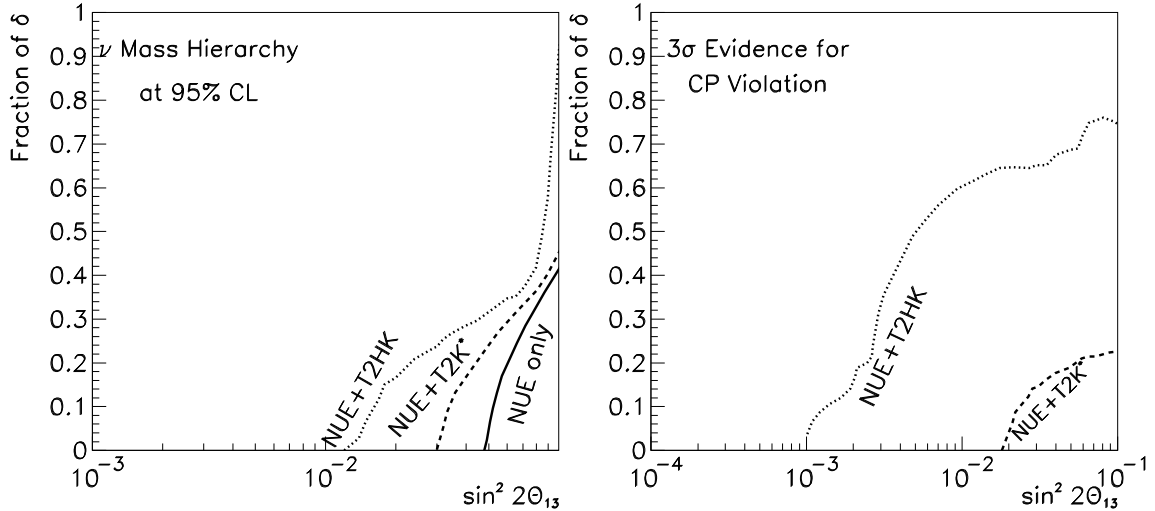


Figure 7: **Case 2: An upgrade to the T2K beam, but no Fermilab Proton Driver.** Regions of parameter space where the mass hierarchy (left) and CP violation (right) can be observed at 95% CL and at 3σ , respectively. NUE, T2K, etc are defined in Table 3.

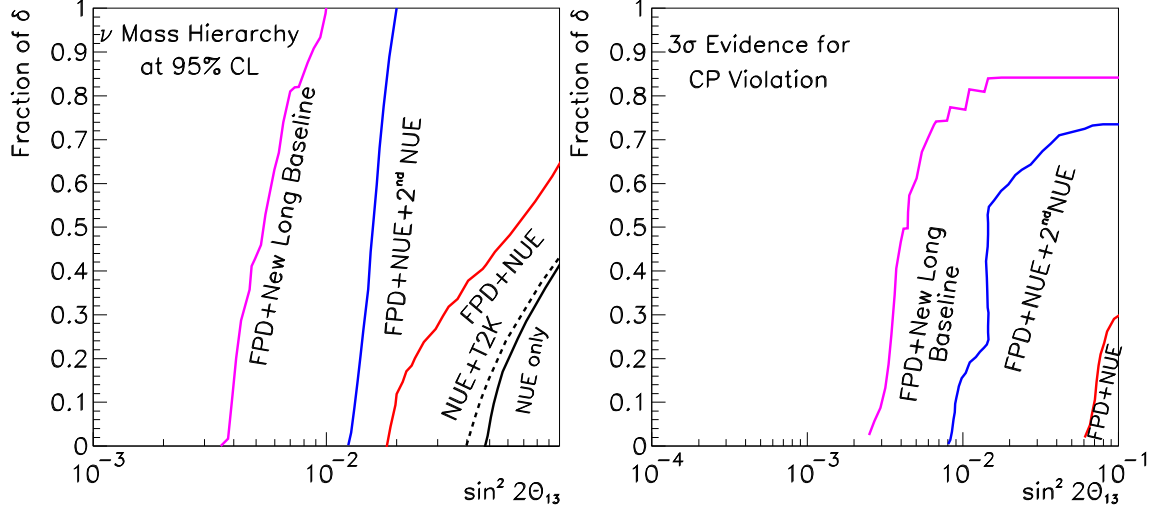


Figure 8: Case 3: A Fermilab Proton Driver, but no upgrade to the T2K beam. Regions of parameter space where the mass hierarchy (left) and CP violation (right) can be observed at 95% CL and at 3σ , respectively. NUE, T2K, etc are defined in Table 3. The addition of T2K data would not significantly change the position of these curves.

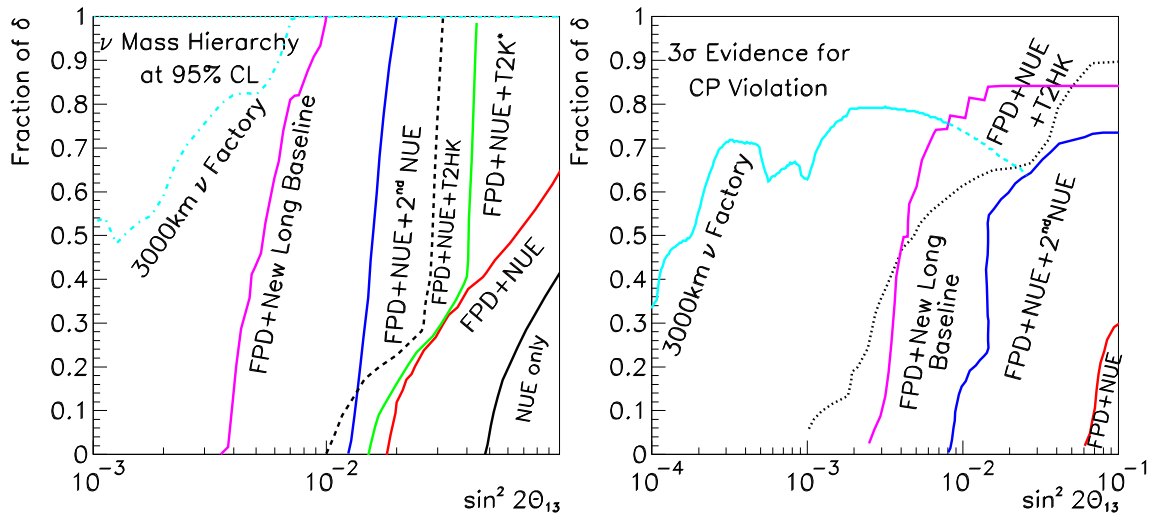


Figure 9: Case 4: Both a Fermilab Proton Driver and an upgraded T2K beam. Regions of parameter space where the mass hierarchy (left) and CP violation (right) can be observed at 95% CL and at 3σ , respectively. NUE, T2K, etc are defined in Table 3.

| Name | Detector Mass (kton) | Proton Power (MW) | Running Time (years) |
|-----------------------------|----------------------|-------------------|---------------------------|
| NUE | 50 | 0.4 | $3\nu + 3\bar{\nu}$ |
| FPD+NUE | 50 | 2.0 | $3\nu + 3\bar{\nu}$ |
| FPD+NUE+2 nd NUE | 50(+50) | 2 | $6(3)\nu + 6(3)\bar{\nu}$ |
| FPD+New Long Baseline | 125 or 500 | $2 + 2$ | $5\nu + 5\bar{\nu}$ |
| T2K | 50 | 0.77 | $3\nu + 3\bar{\nu}$ |
| T2K* | 50 | 4 | $3\nu + 3\bar{\nu}$ |
| T2HK | 500 | 4 | $3\nu + 3\bar{\nu}$ |
| 3000km ν Factory | 50 | 4 | $3\nu + 3\bar{\nu}$ |

Table 3: Summary of the various experiments which are discussed in the text and Figs. 4 and 5. NUE numbers are for the proposed NO ν A detector.

mass hierarchy. NUE would provide some sensitivity to the mass hierarchy, which would be somewhat improved by combining NUE and T2K results.

The second case, where there is no Fermilab Proton Driver but the T2K beam is upgraded, is shown in Fig. 7. We assume that NUE is built, which will provide some sensitivity to the mass hierarchy. In this case, there is some parameter space where CP violation can be seen at 3σ , which expands dramatically if there is a 20-fold increase in detector mass which would happen if Hyper-Kamiokande were to be built. However, there would always be a significant fraction of δ for which there would be an ambiguity due to the uncertain mass hierarchy, which means that a degenerate CP conserving solution may overlap the CP violating solution and destroy the CP violation sensitivity. The T2K upgrades would also extend the sensitivity to the mass hierarchy. However, because the baseline is 295 km, these substantial upgrades make only a modest impact on the mass hierarchy sensitivity for a limited fraction of the δ parameter space.

The third case, shown in Fig. 8, is where there is a Fermilab Proton Driver, but no T2K upgrade. The curves show various options: either running with one or more detectors located at different off axis angles from the NuMI beamline, or with a new long baseline experiment with a new beamline. Note that the Fermilab Proton Driver yields a dramatic improvement in the potential to determine the mass hierarchy, which compares favorably with Case 2. The initial Fermilab Proton Driver experiment would have limited sensitivity to CP violation, but further upgrades to the beamline and detector would provide a significantly improved sensitivity which is again favorable when compared to Case 2.

The fourth case, shown in Fig. 9, is where there is both a Fermilab Proton Driver and an upgraded T2K program. If in the initial program the fluxes are increased, but detectors are not upgraded, then there is some improvement in sensitivity over Case 3, particularly for the mass hierarchy at large $\sin^2 2\theta_{13}$.

In presenting the impact of a Fermilab Proton Driver on the global neutrino program we have featured an off-axis narrow band beam experiment, NUE. Recently a group from Brookhaven has proposed an alternative approach which exploits an

on-axis broad band beam with a long baseline ($L = 2540$ km corresponding to BNL to the Homestake mine) [73]. To understand whether this approach could also be implemented at Fermilab calculations have been made [74] for a baseline of 1290 km, corresponding to FNAL to the Homestake mine. The resulting precision in the $(\sin^2 2\theta_{13}, \delta)$ plane is found to be comparable to or better than the $L = 2540$ km case. Whether the broadband beam concept is better or worse than the off-axis concept depends critically on the assumed background levels for the broadband experiment. A third alternative has been proposed in which a broad energy range is covered by a set of narrow band beams going to the same detector, the tighter energy spread significantly reducing backgrounds. One of these neutrino beams would be produced using the 8 GeV linac beam, and would require the highest practical primary beam power (~ 2 megawatts). Whichever is ultimately preferred, the Fermilab Proton Driver would be able to accommodate any of these alternatives.

In summary, although we do not know the value of θ_{13} or at what point in time its value will be known, we do know that the Fermilab Proton Driver will offer choices that will enable it to provide a critical contribution to the global program. In all the cases considered, without a Fermilab Proton Driver the sensitivity to the neutrino mass hierarchy will be very limited.

3 Neutrino Scattering

While neutrino oscillation experiments probe the physics of neutrino masses and mixing, neutrino scattering experiments probe the interactions of neutrinos with ordinary matter, and enable a search for exotic neutrino properties. A complete knowledge of the role of neutrinos in the Universe in which we live requires a detailed knowledge of neutrino masses, mixing, and interactions.

Our present knowledge of the neutrino and anti-neutrino scattering cross sections in matter is limited. The next generation of approved neutrino scattering experiments, including MINER ν A [75] in the NuMI beamline and MiniBooNE [19] using neutrinos from the Fermilab Booster, are expected to greatly improve our knowledge. In particular, within the next few years we anticipate that precise measurements will be made of neutrino scattering on nuclear targets. However, we will still lack precise measurements of:

- Anti-Neutrino scattering on nuclear targets.
- Neutrino and anti-neutrino scattering on nucleon (hydrogen and deuterium) targets.
- Neutrino-electron scattering.

The anti-neutrino rates per primary proton on target are, depending on energy, a factor of 3-5 less than the neutrino rates. The interaction rates on nucleon targets are an order of magnitude less than the corresponding rates on nuclear targets, and the cross-section for neutrino-electron scattering is considerably smaller than that on nucleons. Hence, beyond the presently approved program, a factor of 10-100 increase in data rates will be required to complete the neutrino and anti-neutrino scattering measurements.

Completing the program of neutrino and anti-neutrino scattering measurements is important for two reasons that will be expanded upon in the following sections.

1. Neutrino scattering experiments can improve our knowledge of the fundamental properties of neutrinos.
2. Neutrino and antineutrino scattering provide a unique tool for probing the structure of matter and obtaining a more complete understanding of the nucleon in general, and its flavor and spin content in particular.

The neutrino scattering program is of interest to a broad community of particle physicists, nuclear physicists, and nuclear-astrophysicists.

3.1 Fundamental Neutrino Properties

Neutrino scattering experiments serve to further our understanding of fundamental neutrino properties. Measurements of neutrino-nucleus cross-sections are needed to constrain the systematic uncertainties of neutrino oscillation experiments. Measurements of neutrino-electron scattering, a process with a robust theoretical cross-section, can probe non-standard neutrino properties and couplings.

3.1.1 Cross-Section Measurements for Oscillation Experiments

To measure neutrino oscillation probabilities it is necessary to know the composition, intensity, divergence, and energy spectrum of the initial beam, and also know all the relevant neutrino and anti-neutrino cross-sections. A well designed “near detector” setup enables the initial beam to be well characterized, and provides cross-section measurements with adequate precision for the oscillation program. In practice it has proved necessary to have more than one type of near detector. The K2K Experiment used both a near detector that replicated the far detector, and additional near detectors optimized to learn more about the underlying cross-sections. The Fermilab long baseline neutrino program is following a similar strategy. The MINOS near detector replicates the far detector, and the MINER ν A detector [75] has been designed to learn more about the underlying cross-sections and nuclear effects.

Neutrino scattering experiments will play a key role in allowing future precision oscillation experiments to reach their ultimate sensitivity. To obtain the most precise value of Δm_{32}^2 (which is eventually required to extract mixing angles and the CP-violating phase) we must better understand and quantify the nuclear processes interposed between the interaction of an incoming neutrino and measurement of outgoing particles in the detector. Extracting mixing parameters such as θ_{13} , and ultimately the neutrino mass hierarchy and CP phase, also requires much better understanding of the neutral current resonant and coherent cross-sections that contribute to the background. The precision measurement of nuclear effects and exclusive cross-sections will provide the necessary foundation for the study of neutrino oscillation with high-luminosity beams at the Fermilab Proton Driver. The unprecedented statistical power will otherwise be compromised by systematic uncertainties from poorly known cross-sections.

The same careful study of cross-sections and nuclear effects must be performed with anti-neutrinos to understand matter effects and CP violation. To approach the same statistical accuracy with anti-neutrinos as with neutrinos, and thus have the same impact on oscillation measurement systematics many more protons on target are needed. This is due to a factor of 1.5 - 2.0 in the number of π^+ to π^- produced and an additional factor of 2.0 to 3.0 in the cross-section ratio. The MINER ν A proposal assumes about 9×10^{20} POT in a 3 ton fiducial volume for neutrino studies. This implies that for those measurements that are statistics limited, one would need $(30 - 50) \times 10^{20}$ POT for an anti-neutrino scattering experiment to approach similar statistical accuracy. The combination of a Fermilab Proton Driver and somewhat larger fiducial volume would make this a feasible experiment.

3.1.2 Neutrino-Electron Scattering

The SM predictions for neutrino-electron elastic scattering have little theoretical uncertainty, and a measurement of $\nu e \rightarrow \nu e$ scattering can therefore be used to search for physics beyond the SM. Since it is now known that neutrinos have non-zero mass, a neutrino magnetic moment becomes a possibility. Within the SM, modified to include finite neutrino masses, neutrinos may acquire a magnetic moment via radiative

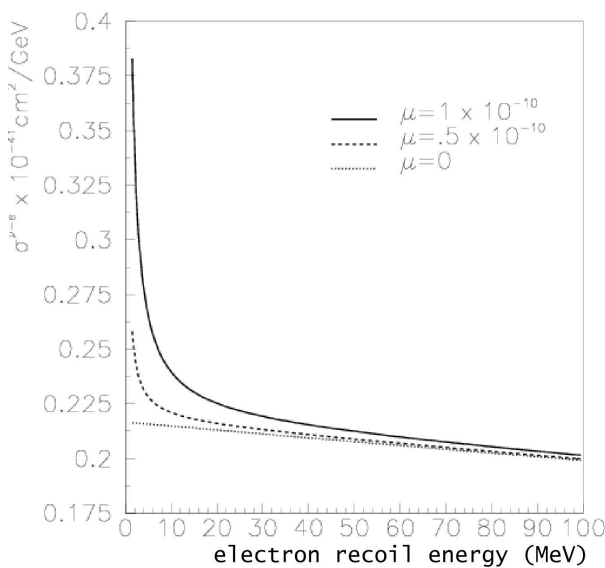


Figure 10: Differential cross section versus electron recoil kinetic energy, T , for $\nu e \rightarrow \nu e$ events. The electroweak contribution is linear in T (bottommost line), while contributions from nonzero neutrino magnetic moments yield sharp rises at low T . The magnetic moment μ is given in units of the Bohr magneton μ_B .

corrections. With $m_\nu = 1$ eV, the resulting magnetic moment would be $\sim 3 \times 10^{-19} \mu_B$ where $\mu_B = e/2m_e$ is the Bohr magneton. This value is too small to be detected. Hence, a search for a neutrino magnetic moment is a search for physics beyond the SM.

The current best limit on the muon neutrino magnetic moment is $\mu_{\nu_\mu} \leq 6.8 \times 10^{-10} \mu_B$ from LSND $\nu_\mu e$ elastic scattering [76]. This sensitivity may be substantially improved by precisely measuring the elastic scattering rate as a function of electron recoil energy. An electromagnetic contribution to the cross section from the magnetic moment will show up as an increase in event rate at low electron recoil energies (see Fig. 10). A high statistics measurement, made possible by the Fermilab Proton Driver, would enable a gain in precision of 10-30 over the LSND measurement. This sensitivity is sufficient to begin to test some beyond-the- Standard-Model predictions (which can be as large as $10^{-11} \mu_B$). The lower neutrino energy means that a beam created by 8 GeV protons (rather than 120 GeV) would be preferred.

3.2 Fundamental Properties of Matter

Neutrinos and anti-neutrinos have only weak interactions making them unique probes of the properties of matter at both the nucleon and nuclear level. With the high statistics available from the Fermilab Proton Driver a variety of high precision measurements become possible.

Parton Distribution Functions

The study of the partonic structure of the nucleon, using the neutrino's weak probe, will complement the on-going study of this subject with electromagnetic probes at Jlab. The unique ability of the neutrino to "taste" only particular flavors of quarks enhances any study of parton distribution functions. With the high statistics and carefully controlled beam systematics from the Fermilab Proton Driver, it should be possible to isolate the contribution of individual quark flavors to the scattering process.

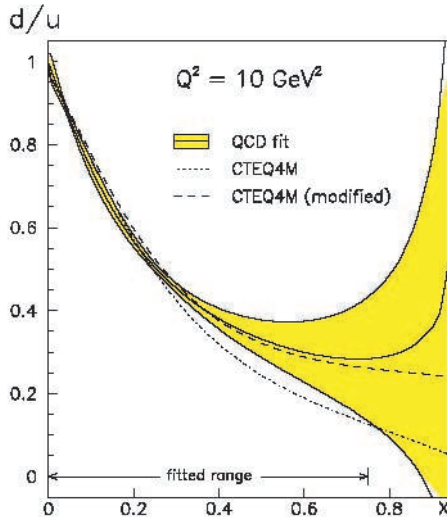


Figure 11: The d/u ratio showing the uncertainty due to nuclear effects in the deuteron. Figure taken from Ref. [77].

Our knowledge of the parton distributions is still very incomplete. Even the valence PDFs are not well known at large x . The ratio of d/u is normally determined by comparing scattering from the proton and neutron. Since no free neutron target exists, the deuteron is used as a neutron target. This makes little difference at small x , but uncertainties in the nuclear corrections become substantial for x larger than about 0.6, and make determination of the ratio essentially impossible for x larger than about 0.8, as shown in Fig. 11. The ratio of d/u can be determined without any nuclear structure effect corrections by using neutrino and anti-neutrino scattering on hydrogen. Only a MW-scale Proton Driver can produce anti-neutrino fluxes sufficiently intense for this measurement to be made.

Generalized Parton Distribution Functions

One of the most exciting developments in the theory of the structure of the nucleon has been the introduction of generalized parton distributions (GPDs) [78–82]. The usual PDFs are sensitive only to the longitudinal momentum distributions of the parton. The GPDs give a more complete picture of the nucleon in which the spatial distribution can be determined as a function of the longitudinal momentum distribution. However, the GPDs are difficult to access experimentally as they require

measurement of exclusive final states. The most promising reaction to date is deeply virtual Compton scattering (DVCS), i.e. $p(e, e'\gamma p)$. These measurements are either underway or planned at JLab. However, a complete determination of the GPDs requires flavor separation which can only be accomplished using neutrinos and anti-neutrinos. Although MINER ν A will measure GPDs on carbon, nuclear effects will ensure that this will be considerably inferior to a measurement on the proton. A true GPD measurement would require $p(\bar{\nu}, \mu\gamma n)$ and $n(\nu, \mu\gamma p)$ reactions using hydrogen and deuteron targets. Estimates for this “weak DVCS” process are currently being made by A. Psaker [83]. The CC cross section at 2 GeV is of order 10^{-41}cm^2 and the NC about 10 times smaller. These small cross sections will clearly require the higher intensity neutrino beams that the Fermilab Proton Driver could deliver.

Strange Quarks and the Spin Structure of the Nucleon

The NC elastic scattering of neutrinos and anti-neutrinos on nucleons ($\nu N \rightarrow \nu N$, $\bar{\nu} N \rightarrow \bar{\nu} N$) provides information about the spin structure of the nucleon. In particular, these scattering processes are sensitive to the isoscalar spin structure that results from strange quark contributions. Determination of the strange quark contribution to the nucleon Δs has been a major component of the JLab program [84], but such measurements are strongly influenced by theoretical assumptions. A precise measurement of NC elastic scattering would provide a direct measurement of Δs that is insensitive to theoretical assumptions [85]. The ideal measurement would be of the $(\nu p \rightarrow \nu p)/(\nu n \rightarrow \mu p)$ cross-section ratio on a deuterium target. The ultimate goal in this program requires measuring NC elastic scattering with both neutrinos and anti-neutrinos, with a large event sample, on *nucleon* targets, which will require a megawatt-scale proton source to produce a narrow band neutrino beam of sufficiently high intensity. Note also that this measurement should be done using the lower energy neutrino beam from 8 GeV protons (rather than 120 GeV). These lower energies minimize the background of neutrino induced neutrons from the surrounding environment as well as feed down backgrounds from other neutrino interactions.

Elastic Form Factors

The distributions of charge and magnetism within the nucleus can be parameterized using two elastic form factors: the electric form factor G_E and the magnetic form factor G_M . For many years it was assumed that both the charge and magnetic distributions fall exponentially. However, precision measurements at JLab [86, 87] have shown that this is not the case, with the charge appearing to have a broader spatial distribution than that of magnetism. Although the reason for this is not understood, it does appear to be an indication of angular momentum between the quarks. To understand this more deeply it is desirable to precisely measure the weak form factor. This can be done through parity violation in electron-nucleon scattering, with limited precision. In neutrino-nucleon elastic (or quasi-elastic) scattering nearly half the cross section is due to the weak form factor, making it a much better probe. Proposed measurements of the weak form factor (e.g. the MINER ν A experiment)

use scattering from nucleons in nuclei. Although the statistical precision will be reasonably good, there is an uncertainty in both extracting the form factor from scattering from a bound nucleon due to final state interactions and other conventional effects, as well as the possibility of modification of the form factor by the nuclear medium. Thus, measurement of the form factor using neutrino scattering on hydrogen and deuterium is essential. This will require the intensity available at a megawatt-scale Proton Driver.

Duality and Resonance Production

Although QCD appears to provide a good description of the strong interaction, we have a very poor understanding of the transition from the domain where quarks and gluons are the appropriate degrees of freedom to the domain best described using baryons and mesons. In the region of modest Q^2 (1-10 GeV 2) the scattering of electrons on nucleons is dominated by resonance production, and can also be described using the same formalism as DIS. Experiments at JLab [88] have, quite unexpectedly, found that the F_2 structure function measured in the resonance region closely follows that measured in the DIS region. The phenomenon, called quark-hadron duality, has also been observed in other processes, such as e^+e^- annihilation into hadrons. The origins of duality are not well understood [89–96]. It is expected to exist for neutrino scattering, though it may manifest itself quite differently. Of particular interest would be a measurement of the ratio of neutron to proton neutrino structure functions at large x . The next decade of experiments should provide some information on the validity of duality using neutrinos. However, high precision measurements using anti-neutrinos and nucleon (hydrogen and deuterium) targets will be required in order to fully explore the origins of duality and hence the high fluxes of the Fermilab Proton Driver will be needed.

Strange Particle Production

Measurements of the production of strange mesons and hyperons in neutrino NC and CC processes (e.g. $\nu_\mu n \rightarrow \mu^- K^+ \Lambda^0$ and $\nu_\mu p \rightarrow \nu_\mu K^+ \Lambda^0$) provide input to test the theoretical models of neutral current neutrino induced strangeness production [97,98]. In addition, such strangeness production is a significant background in searches for proton decay based on the SUSY-inspired proton decay mode $p \rightarrow \nu K^+$. The existing experimental data on these channels consists of only a handful of events from bubble chamber experiments. There are plans to measure these reactions using the existing K2K data and the future MINER ν A data. MINER ν A will collect a large sample ($\approx 10,000$) of fully constrained $\nu_\mu n \rightarrow \mu^- K^+ \Lambda^0$ events. However, the anti-neutrino measurements will require a more intense (megawatt-scale) proton source.

4 The Broader Proton Driver Physics Program

In the past, high precision measurements at low energies have complemented the experimental program at the energy frontier. These low energy experiments not only probe mass scales that are often beyond the reach of colliders, but also provide complementary information at mass scales within reach of the energy frontier experiments. Examples of low energy experiments that have played an important role in this way are muon ($g - 2$) measurements, searches for muon and kaon decays beyond those predicted by the SM, and measurements of rare kaon processes. A summary of the sensitivity achieved by a selection of these experiments is given in Fig. 12. It seems likely that these types of experiment will continue to have a critical role as the energy frontier moves into the LHC era. In particular, if the LHC discovers new physics beyond the SM, the measurement of quantum corrections that manifest themselves in low energy experiments would be expected to help elucidate the nature of the new physics. If no new physics is discovered at the LHC then precision low energy experiments may provide the only practical way of advancing the energy frontier beyond the LHC in the foreseeable future.

| $\Delta G = 0 \text{ or } 2$ | Experimental Result (90% CL) | M or ΔM Limit |
|--------------------------------------|---|---|
| | $B(K_L^0 \rightarrow \mu^\pm e^\mp) < 4.7 \times 10^{-12}$ | $150 \text{ TeV}/c^2$ |
| | $B(K^+ \rightarrow \pi^+ \mu^+ e^-) < 4 \times 10^{-11}$ | $31 \text{ TeV}/c^2$ |
| | $B(K_L^0 \rightarrow \pi^0 \mu^\pm e^\mp) < 3.2 \times 10^{-10}$ | $37 \text{ TeV}/c^2$ |
| $\Delta G = 1$ | | |
| | $B(\mu^+ \rightarrow eeee) < 1 \times 10^{-12}$ | $86 \text{ TeV}/c^2$ |
| | $B(\mu^+ \rightarrow e^+ \gamma) < 1.2 \times 10^{-11}$ | $21 \text{ TeV}/c^2$ |
| | $\frac{\Gamma(\mu^- A \rightarrow e^- A)}{\Gamma(\mu^- A \rightarrow \nu A)} < 6.1 \times 10^{-13}$ | $365 \text{ TeV}/c^2$ |
| $\Delta G = \pm 2$ | | |
| | $\Delta M_K < 3.5 \times 10^{-12} \text{ MeV}/c^2$ | $400 \text{ TeV}/c^2$ |

Figure 12: Current limits on Lepton Flavor Violating processes and the mass scales probed by each process. The upper box is for kaon decays, which involve a change of both quark flavor and lepton flavor. The bottom box is for muon decays, which involve only lepton flavor change. The lower limit on the mass scale is calculated assuming the electroweak coupling strength.

| Measurement | Sensitivity | |
|---------------------------------|------------------------------|------------------------------|
| | Present or Near Future | Fermilab Proton Driver |
| EDM d_μ | $< 3.7 \times 10^{-19}$ e-cm | $< 10^{-24} - 10^{-26}$ e-cm |
| $(g - 2) \sigma(a_\mu)$ | 0.2 – 0.5 ppm | 0.02 ppm |
| BR($\mu \rightarrow e\gamma$) | $\sim 10^{-14}$ | $\sim 10^{-16}$ |
| $\mu \rightarrow e$ R | $\sim 10^{-16}$ | $\sim 10^{-19}$ |

Table 4: A comparison of the present or near future sensitivities of the muon experiments considered in the text to those attainable with a Fermilab Proton Driver.

4.1 Muon Physics

Solar-, atmospheric-, and reactor-neutrino experiments have established Lepton Flavor Violation (LFV) in the neutrino sector, which suggests the existence of LFV processes at high mass scales. Depending on its nature, this new physics might also produce observable effects in rare muon processes. Furthermore, CP violation in the charged lepton sector, revealed for example by the observation of a finite muon Electric Dipole Moment (EDM), might be part of a broader baryogenesis via leptogenesis picture. Hence, the neutrino oscillation discovery enhances the motivation for a continuing program of precision muon experiments. In addition, the expectation that there is new physics at the TeV scale also motivates a new round of precision muon experiments. LFV muon decays and the muon anomalous magnetic moment $a_\mu = (g - 2)/2$ and EDM are sensitive probes of new dynamics at the TeV scale. In general, with sufficient sensitivity, these experiments would help elucidate the nature of new physics observed at the LHC. As an example, in SUSY models the muon $(g - 2)$ and EDM are sensitive to the diagonal elements of the slepton mixing matrix, while LFV decays are sensitive to the off-diagonal elements. If SUSY is observed at the LHC we will probably have some knowledge of the slepton mass scale. Precision muon experiments would provide one of the cleanest measurements of $\tan \beta$ and of the new CP violating phases. It is possible that no new physics will be observed at the LHC. In this case precision muon experiments might provide, for the foreseeable future, one of the few practical ways to probe physics at higher mass scales. Note that the Brookhaven $(g - 2)$ Collaboration have reported a value for $(g - 2)$ that is 2.7 standard deviations away from the SM prediction. Noting that the muon $(g - 2)$ is sensitive to any new heavy particles that couple to the muon, it is possible that the current measurements are providing an early indication of the existence of new TeV-scale particles. Higher precision measurements are well motivated.

In the following, after describing the muon source at the Fermilab Proton Driver, the expected sensitivity of muon EDM, $(g - 2)$, and LFV decay experiments is discussed. Table 4 summarizes the expected improvements in sensitivity.

4.1.1 The Muon Source

Low energy high precision muon experiments require high intensity beams. Since most of the 8 GeV Fermilab Proton Driver beam from the SC linac would not be used to fill

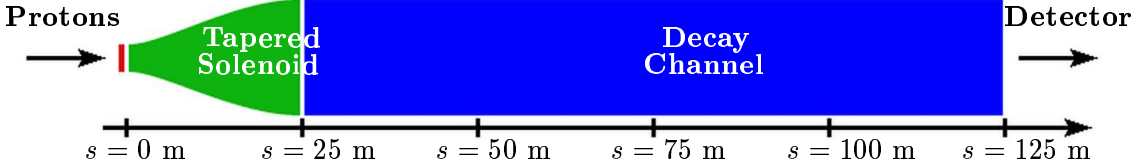


Figure 13: Schematic of the solenoid-based muon source discussed in the text. The performance of this channel has been simulated using the MARS code.

the MI, it would be available to drive a high intensity muon source. In addition to high intensity, precision muon experiments also require an appropriate bunch structure, which varies with experiment. In the post-collider period it might be possible to utilize the Recycler Ring to repackage the 8 GeV proton beam, yielding a bunch structure optimized for each experiment. The combination of Proton Driver plus Recycler Ring would provide the front-end for a unique muon source with intensity and flexibility that exceed any existing facility.

The Recycler is an 8 GeV storage ring in the MI tunnel that can run at the same time as the MI. The beam from the Fermilab Proton Driver SC linac that is not used to fill the MI could be used to fill the Recycler Ring approximately ten times per second. The ring would then be emptied gradually in the 100 ms intervals between linac pulses. Extraction could be continuous or in bursts. For example, the Recycler Ring could be loaded with one linac pulse of 1.5×10^{14} protons every 100 ms, with one missing pulse every 1.5 seconds for the 120 GeV MI program. This provides $\sim 1.4 \times 10^{22}$ protons at 8 GeV per operational year (10^7 seconds). In the Recycler each pulse of 1.5×10^{14} protons can be chopped into 588 bunches of 0.25×10^{12} protons/bunch with a pulse width of 3 ns. A fast kicker allows for the extraction of one bunch at a time. The beam structure made possible by the Proton Driver linac and the Recycler Ring is perfect for $\mu \rightarrow e$ conversion experiments, muon EDM searches and other muon experiments where a pulsed beam is required. Slow extraction from the Recycler Ring for $\mu \rightarrow e\gamma$ and $\mu \rightarrow 3e$ searches is also possible.

The performance of the strawman muon source shown in Fig. 13 has been simulated using the MARS code. The evolution of the pion and muon fluxes down the decay channel is shown in Table 5. The scheme will yield ~ 0.2 muons of each sign per incident 8 GeV proton. With 1.4×10^{22} protons at 8 GeV per operational year (corresponding to ~ 2 megawatts) this would yield $\sim 3 \times 10^{21}$ muons per year. This muon flux greatly exceeds the flux required to make progress in a broad range of muon experiments (see Fig. 14). However, the muons at the end of the decay channel have low energy, a large momentum spread, and occupy a large transverse phase space. Without further manipulation their utilization will be very inefficient. The interface between the decay channel and each candidate experiment has yet to be designed. In Japan a Phase Rotated Intense Slow Muon Source (PRISM) based on an FFAG ring that reduces the muon energy spread (phase rotates) is being designed. This phase rotation ring has a very large transverse acceptance (800π mm-mrad) and a momentum acceptance of $\pm 30\%$ centered at 500 MeV/c. PRISM reduces the momentum and momentum spread to 68 MeV/c and $\pm 1 - 2\%$ respectively. Hence, a

| Experiment | Sensitivity Goal | $\int I_\mu dt$ | I_0/I_m | δT [ns] | ΔT [μs] | p_μ [MeV] | $\Delta p_\mu/p_\mu$ [%] |
|---------------------------|-----------------------|-----------------|--------------|-----------------|------------------------|---------------|--------------------------|
| $\mu A \rightarrow eA$ | 10^{-20} | 10^{21} | $< 10^{-10}$ | < 100 | > 1 | < 80 | < 5 |
| $\mu \rightarrow e\gamma$ | 10^{-16} | 10^{17} | n/a | n/a | n/a | < 30 | < 10 |
| $\mu \rightarrow eee$ | 10^{-16} | 10^{17} | n/a | n/a | n/a | < 30 | < 10 |
| τ_μ | 0.5 ppm | 10^{15} | $< 10^{-5}$ | 100 | > 20 | 30 | < 10 |
| $(g - 2)$ | 0.02 ppm | 10^{15} | $< 10^{-7}$ | < 50 | $> 10^3$ | 3100 | < 2 |
| EDM | $10^{-24} e \cdot cm$ | 10^{16} | $< 10^{-6}$ | < 50 | $> 10^3$ | < 1000 | < 2 |

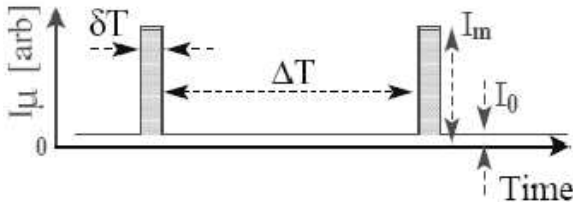


Figure 14: Beam requirements for new muon experiments. Shown are the expected sensitivity goals at the time of the Fermilab Proton Driver, the number of muons needed to achieve that sensitivity, the muon suppression between pulses, the length and separation of pulses and the momentum spread of the muon beam.

PRISM-like ring downstream of the decay channel might accept a significant fraction of the muon spectrum and provide a relatively efficient way to use the available muon flux. Explicit design work must be done to verify this, but it should be noted that a muon selection system that utilizes only 1% of the muons available at the end of the decay channel will still produce an adequate muon flux for most of the cutting-edge experiments described in the following sections.

Finally, a new 8 GeV multi-MW Proton Driver at Fermilab, together with an appropriate target, pion capture system, decay channel, and phase rotation system could provide the first step toward a Neutrino Factory based on a muon storage ring. The additional systems needed for a neutrino factory are a cooling channel (to produce a cold muon beam occupying a phase space that fits within the acceptance of an accelerator) an acceleration system (which perhaps would use the Proton Driver SC linac), and a storage ring with long straight sections.

4.1.2 Electric Dipole Moment

Electric Dipole Moments violate both parity (P) and time reversal (T) invariance. If CPT conservation is assumed, a finite EDM provides unambiguous evidence for CP violation. In the SM EDMs are generated only at the multi-loop level, and are predicted to be many orders of magnitude below the sensitivity of foreseeable experiments. Observation of a finite muon EDM (d_μ) would therefore provide evidence for new CP violating physics beyond the SM. CP violation is an essential ingredient

| | $s = 25$ m | $s = 50$ m | $s = 75$ m | $s = 100$ m | $s = 125$ m |
|-----------|------------|------------|------------|-------------|-------------|
| μ^+/P | 0.16 | 0.20 | 0.21 | 0.21 | 0.22 |
| μ^-/P | 0.16 | 0.20 | 0.21 | 0.21 | 0.21 |
| π^+/P | 0.095 | 0.051 | 0.030 | 0.020 | 0.014 |
| π^-/P | 0.087 | 0.044 | 0.025 | 0.016 | 0.011 |

Table 5: The number of charged particles in the beam per incident 8 GeV primary proton as a function of the distance downstream from the target. These numbers are computed using the MARS code. The normalization corresponds to a 2 megawatt Proton Driver.

of almost all attempts to explain the matter-antimatter asymmetry of the Universe. However, the measured CP violation in the quark sector is known to be insufficient to explain the observed matter-antimatter asymmetry. Searches for new sources of CP violation are therefore well motivated.

A number of extensions to the SM predict new sources of CP violation. Supersymmetric models in which finite neutrino masses and large neutrino mixing arise from the seesaw mechanism provide one example. In these models d_μ can be significant. There are examples in which the interactions responsible for the masses of right-handed Majorana neutrinos produce values of d_μ as large as 5×10^{-23} e-cm. This is well below the present limit $d_\mu < 3.7 \times 10^{-19}$ e-cm, but would be within reach of a new dedicated experiment at a high intensity muon source. The muon EDM group has proposed an experiment at JPARC to obtain a sensitivity of 10^{-24} e-cm. This sensitivity would still be limited by statistics. Higher muon intensities would help, although the measurement would also be rate limited. To obtain a sensitivity of $O(10^{-26})$ e-cm would require an improved beam structure with many short pulses, each separated by at least 500 μ s. Hence, depending on the fate of the JPARC proposal, a muon EDM experiment at a Fermilab Proton Driver would be designed to obtain a sensitivity somewhere in the $10^{-24} - 10^{-26}$ e-cm range.

4.1.3 Muon ($g - 2$)

The Brookhaven ($g - 2$) Collaboration has reported a value that is 2.7 standard deviations from the SM prediction. This could be an early indication of new physics at the electroweak symmetry breaking scale. Physics that would affect the value of ($g - 2$) include muon substructure, anomalous gauge couplings, leptoquarks, and SUSY. For example, in a minimal supersymmetric model with degenerate sparticle masses the contribution to $a_\mu = (g - 2)/2$ could be substantial, particularly for large $\tan\beta$. With degenerate SUSY masses, the estimated range of masses that correspond to the observed a_μ are 100 - 450 GeV for $\tan\beta = 4 - 40$. Hence the present ($g - 2$) experiment is probing the mass range of interest for electroweak symmetry breaking. With further data taking the BNL experiment might be able to improve sensitivity

by a factor of a few. To make progress beyond this will require either an upgraded storage ring or a new ring, and a higher intensity muon source at, for example, the Fermilab Proton Driver.

The current measurement of a_μ is accurate to $0.46 \text{ (stat)} \pm 0.27 \text{ (sys) ppm}$. A proposed upgrade to the current program could increase the overall precision from 0.5 ppm to 0.2 ppm. A new experiment at the Fermilab Proton Driver might improve this precision by an order of magnitude, which would be accomplished by reducing the systematic error by a factor of seven and increasing the statistical sample by a factor of 200. To fully exploit this improvement in experimental precision a corresponding improvement in the precision of the theoretical prediction will be required, which will need a very high precision measurement of hadronic production in e^+e^- collisions from threshold to $\sim 2.5 \text{ GeV}$.

4.1.4 Rare Muon Decays

If a negative muon is stopped in a target it will be captured by an atom and then cascade down to the $1s$ atomic level. In the SM the muon will either decay in orbit or will be captured by the nucleus with the emission of a neutrino. In LFV models beyond the SM the muon can also be converted into an electron in the field of the nucleus ($\mu \rightarrow e$ conversion) or can undergo non-SM decays ($\mu \rightarrow e\gamma$, $\mu \rightarrow eee$, ...). If the SM is extended to include the seesaw mechanism with right-handed neutrinos in the mass range 10^{12} to 10^{15} GeV , the predicted LFV decay branching ratios are unobservably small. However in SUSY seesaw models, the resulting LFV decay branching ratios can be significant. The predicted branching ratios depend upon the origin of SUSY breaking. Muon LFV decay searches therefore place constraints on SUSY breaking schemes.

Consider first $\mu \rightarrow e\gamma$. The present limit on the decay branching ratio is 1.2×10^{-11} . Within the context of SUSY models, this limit already constrains the viable region of parameter space. The MEG experiment at PSI is expected to reach a branching ratio sensitivity of 10^{-14} by the end of the decade. The MEG measurement will provide constraints on SUSY parameter space complementary to those obtained by the LHC experiments. If MEG observes $\mu \rightarrow e\gamma$ then both a higher statistics experiment and new searches for other non-SM decay modes will be well motivated. If MEG only obtains a limit, further progress will also require a more sensitive experiment. In either case, a $\mu \rightarrow e\gamma$ experiment at a new Fermilab Proton Driver would provide a way forward provided a high sensitivity experiment can be designed to exploit higher stopped muon rates. Progress will depend upon improvements in technology to yield improved background rejection and higher rate capability. To illustrate the possible gains in the $\mu \rightarrow e\gamma$ sensitivity consider an experiment that uses pixel detectors to track both the decay positron and the electron-positron pair from the converted photon. It has been shown that if BTeV pixel technology is used in an idealized geometry with 10% of the coverage of the old MEGA experiment, then a sensitivity comparable to the expected MEG sensitivity might be obtained at a beamline of the sort to be used by the BNL MECO experiment. The main limitation in using BTeV pixel technology would come from scattering in the fairly thick

detectors. We can anticipate the development of much thinner pixel detectors. If the pixel thickness can be reduced by a factor of 10, coverage increased to 50% of the MEGA coverage, and the readout rate improved by a factor of 20, then the resulting single event sensitivity would be improved by about two orders of magnitude.

Now consider $\mu \rightarrow e$ conversion. Within the context of some SUSY extensions to the SM, the $\mu \rightarrow e$ conversion rate is related to the $\mu \rightarrow e\gamma$ branching ratio:

$$\Gamma(\mu \rightarrow e) \sim 16\alpha Z^4 Z_{eff} |F(q2)|^2 BR(\mu \rightarrow e\gamma) \quad (5)$$

where Z is the proton number for the target nucleus, Z_{eff} is the effective charge, and $F(q2)$ is the nuclear form factor. The $\mu \rightarrow e$ conversion rate normalized to the muon capture rate in Ti is then given by:

$$R(\mu^- \rightarrow e^- Ti) \sim 6 \times 10^{-3} BR(\mu \rightarrow e\gamma) \quad (6)$$

The prediction is model dependent, and hence searches for both $\mu \rightarrow e\gamma$ and $\mu \rightarrow e$ conversion are well motivated. The apparent suppression of the $\mu \rightarrow e$ conversion rate with respect to the $\mu \rightarrow e\gamma$ decay rate is in practice compensated by the higher sensitivity achievable for the conversion experiments. At BNL the MECO experiment is expected to achieve a sensitivity of $O(10^{-17})$ in the coming decade. In the longer term the PRIME experiment has been proposed at JPARC to improve the sensitivity to $O(10^{-19})$. Proton economics may well determine the fate of PRIME. If PRIME is not able to proceed at JPARC it might be accommodated at the Fermilab Proton Driver. If PRIME does proceed in Japan, a further generation experiment might be justified, but its design would presumably need to benefit from lessons learned with MECO and PRIME.

4.2 Other Potential Opportunities

A Fermilab Proton Driver that would provide high intensity beams at both MI energies and at 8 GeV would offer tremendous flexibility for the future physics program, and would enable a vigorous experimental endeavor that extends into and beyond the next two decades. In addition to supporting experiments that exploit lepton beams (neutrinos, anti-neutrinos, and muons), a Fermilab Proton Driver could support a variety of experiments using secondary hadron beams. Although the possibilities have not all been explored, some specific illustrative examples using kaon, pion, neutron, and antiproton beams have been considered.

4.2.1 Kaon Experiments using the MI Beam

Many crucial features of the quark-flavor sector, such as the nature of the couplings, can only be probed indirectly using rare decays. Examples from the past include the flavor changing neutral current (FCNC) suppression via the GIM mechanism and CP violation, both discovered with K-decays. Of particular importance are the ultra-rare FCNC modes $K^+ \rightarrow \pi^+ \nu \bar{\nu}$ and $K_L \rightarrow \pi^0 \nu \bar{\nu}$. The SM expectations for the associated branching ratios are at the $3 - 7 \times 10^{-11}$ level. These decays probe quark flavor

physics in $s \rightarrow d$ transitions. The $K \rightarrow \pi\nu\nu$ modes are ideally suited for this purpose since they are predicted in the SM with high theoretical accuracy. The intrinsic theoretical uncertainty on $\text{BR}(K_L \rightarrow \pi^0\nu\nu)$ is $< 1\%$ and it is expected to reach 6% for $\text{BR}(K^+ \rightarrow \pi^+\nu\nu)$, where the charm quark mass uncertainty dominates. The variety of conceivable new physics scenarios involving $K \rightarrow \pi\nu\nu$ is very large. Within many supersymmetric models, enhancements of between 3 and 10 times larger than SM expectation are possible [99–101]. In minimal flavor violation models, an agreement of $\text{BR}(K_L \rightarrow \pi^0\nu\nu)$ with the SM prediction at the 1% level would constrain the new physics scale to exceed 12 TeV [102].

The world sample of $K^+ \rightarrow \pi^+\nu\nu$ consists of 3 candidate events observed by the combined BNL-E787 and BNL-E949 experiments. The experimental central value for the branching ratio is $1.5^{+1.3}_{-0.9} \times 10^{-10}$, consistent with the SM expectation. There are currently no observed candidates for $K_L \rightarrow \pi^0\nu\nu$. A new generation of experiments has been proposed to observe 50-100 of each of these decay modes within the next 10 years. In the K_L sector, the initiatives are KOPIO at BNL, and KEK391a and the follow-up experiment at JPARC (LOI-05). In the K^+ sector, the initiatives are JPARC-LOI-04, NA48/3 at CERN, and P940 at Fermilab. In the Proton Driver era, assuming the presently proposed experiments meet their 50-100 event goal, a reasonable next goal would be to carry out measurements at the 1000 event level. The near term experiments are already pushing the limit of detector technology and so progress will require improvements in detection technique. Assuming this is the case the required number of protons on target can be estimated by assuming a KAMI-like beam line and detector for the $K_L \rightarrow \pi^0\nu\nu$ case, and using efficiency numbers from the KAMI proposal. For the $K^+ \rightarrow \pi^+\nu\nu$ case, similar quantities can be extrapolated from the P940 proposal. The required numbers of protons on target are given in Table 6.

| Mode | Sample Size | Physics Measurement | POT |
|-------------------------------|----------------|--------------------------------------|---------------------|
| $K^+ \rightarrow \pi^+\nu\nu$ | 1000 | 3% of $ V_{ts} * V_{td} $ | $1.5 \cdot 10^{20}$ |
| $K_L \rightarrow \pi^0\nu\nu$ | 1000 | 1.5% of $\text{Im}(V_{ts} * V_{td})$ | $1.6 \cdot 10^{21}$ |
| $K_L \rightarrow \pi^0e^+e^-$ | $2 \cdot 10^4$ | 10% of $\text{Im}(V_{ts} * V_{td})$ | $2.5 \cdot 10^{20}$ |

Table 6: Desired data sample sizes for various kaon physics measurements in the Proton Driver era, and the associated number of protons on target (POT) needed.

Recently two additional decay modes have received attention: $K_L \rightarrow \pi^0ee$ and $K_L \rightarrow \pi^0\mu\mu$. These decay modes are fully reconstructible, and therefore are significantly easier to identify than $K \rightarrow \pi\nu\nu$. There are no large backgrounds that could "feed-down" and fake the signal. The only serious backgrounds are $K_L \rightarrow ee\gamma\gamma$ and $\mu\mu\gamma\gamma$ which occur with a branching ratio of about 10^{-7} and can be reduced by kinematic cuts to obtain an effective residual background level of $\sim 10^{-10}$. Although this exceeds the expected signal by an order of magnitude, the background is flat over the signal region and with sufficient statistics the signal peaks would enable extraction of the branching ratios.

4.2.2 Pion Experiments using the 8 GeV Beam

Pion experiments can provide precision tests of the SM, and help provide a better understanding of the theory of strong interactions. Pion experiments at the Fermilab Proton Driver would use the 8 GeV beam and only need a power of 0.5 megawatts.

Pions are the lightest hadrons. Their decay modes are few and simple, and they therefore provide an exquisite laboratory for testing fundamental symmetries. It is generally agreed that the next important step in pion decay physics is to accurately measure the branching ratio of the decay $\pi^+ \rightarrow e^+\nu(\gamma)$ (π_{e2}) and normalize it to $\pi^+ \rightarrow \mu^+\nu(\gamma)$ ($\pi_{\mu 2}$). The double ratio $\text{BR}(\pi_{e2})/\text{BR}(\pi_{\mu 2})$ is theoretically clean, probes e- μ universality in weak charged decays, and is predicted [103] in the Standard Model to have a value of $(1.2356 \pm 0.0001) \times 10^{-4}$. Beyond-the-SM scenarios typically preserve lepton universality in weak charged decays, and so it is believed to be a deeply fundamental symmetry. The current world average of the double ratio is $(1.230 \pm 0.004) \times 10^{-4}$. In comparison with lepton universality tests in τ -decays or W-decays, the pion system's experimental precision is $3 - 10\times$ better and is unlikely to be surpassed.

In addition, the π_{e2} measurement provides the normalization for measurements of the decay $\pi^+ \rightarrow e^+\nu_e\pi^0$ decays (π_β). The uncertainty on the π_{e2} measurements dominate the external systematic uncertainties on the π_β measurement. This is of interest because the CKM matrix element V_{ud} can be extracted cleanly from π_β measurements. The current best π_β measurement [104] yields $V_{ud} = 0.9728(30)$. The world average is $V_{ud} = 0.9738(5)$, which is dominated by measurements from super-allowed nuclear decays. However, in the future, improved π_β measurements would allow a theoretically cleaner extraction of V_{ud} , and improved precision provided the statistical and systematic uncertainties can be decreased. Finally, other rare pion decay modes that provide opportunities for searches for new physics are $\pi^0 \rightarrow 3\gamma$, $\pi^0 \rightarrow 4\gamma$, and $\pi^0 \rightarrow \nu\nu$.

The PIBETA experiment at PSI is the current state-of-the-art charged pion decay experiment. PIBETA uses stopped pions. Neutral pion decays are studied using the charge-exchange reaction $\pi^- p \rightarrow \pi^0 n$. It is believed that the decay-at-rest technique is now at its systematic limit. At a Proton Driver, progress could be made by using decay-in-flight techniques.

Light meson and baryon spectroscopy probes the confinement and symmetry properties of QCD. Beyond the usual meson and baryon states, QCD predicts exotic bound configurations of quarks and gluons which include hybrids (e.g. $q\bar{q}g$ and q^3g), pure gluon states (e.g. g^2 and g^3), and multiquark states ($q^2\bar{q}^2$, $q^4\bar{q}$, ...). Only a small fraction of these exotic states have been observed. Observation of these states, together with measurements of their masses and widths, and determination of their quantum numbers, is needed to compare to the predictions of lattice gauge theory, flux tube models, etc. The spectrum of $q\bar{q}$ mesons is well known below 1.5 GeV. Above 1.5 GeV the low angular momentum states are poorly known. This is the region where many exotic states are expected. For example, lattice gauge theory calculations predict glue balls with masses from 2 - 5 GeV.

Our knowledge of the baryon spectrum is also incomplete. The only reasonably

well-known excited light baryon state is the D(1232), whose properties are known to $\sim 5\%$. The properties of a few other excited states, the lowest in each partial wave, are known to 30%. Properties of other ‘known’ states have much larger uncertainties. Therefore higher precision information is needed and missing states must be sought in $N\pi$, ΛK , ΣK scattering experiments.

The nuclear physics community has invested heavily in experimental and theoretical programs aimed at better understanding QCD. The flagship DOE nuclear physics program for spectroscopy currently uses the electromagnetic beam facilities at JLab. However, since the production mechanisms for the various exotic states are not well understood, it is important to use different types of beam. Indeed, the electromagnetic probes available at JLab cannot be analyzed without accounting for the hadronic intermediate states. Hence, pion beam experiments at an upgraded Proton Driver would permit progress in light meson and hadron spectroscopy that would complement the JLab program. The measurements would also provide tests of lattice QCD, and are therefore of interest to the particle physics community. The beam and detector requirements for meson and baryon spectroscopy studies are quite modest. The low energy secondary pion and kaon beams derived from the 8 GeV primary proton beam would be used. A high duty cycle would be desirable, and hence a bunch stretcher would be required.

4.2.3 Neutron Experiments using the 8 GeV Beam

High power proton beams of a few GeV can produce copious numbers of spallation neutrons. A Fermilab Proton Driver operating at 8 GeV and 2 megawatts could produce neutron beams with an intensity that is comparable to those from the most intense neutron sources in the world. The Fermilab Proton Driver could therefore support one or more specialized neutron experiments that, because of their requirements (e.g. pulse structure needs), are either unlikely to be supported at existing or planned neutron spallation facilities, or could be performed much better at the Fermilab Proton Driver. Some examples of candidate experiments that are of particular interest to particle physicists are searches for neutron-antineutron oscillations, searches for a neutron electric dipole moment (EDM), and precision measurements of the neutron lifetime.

Neutron-antineutron oscillations require baryon number violation, with a change in baryon number of two units. Searches for neutron-antineutron oscillations are therefore complementary to searches for nucleon decay, which requires a change in baryon number of one unit. Thus, neutron-antineutron oscillation searches provide a unique test of the fundamental stability of matter. The current limit on a possible transition time between the free neutron and antineutron is ~ 10 years [105]. This sensitivity is essentially statistics limited. Since there are no suitable neutron sources available for a new experiment, at present there are no concrete plans to improve this sensitivity. The Fermilab Proton Driver could provide a cold neutron source with an average flux equivalent to that of a ~ 20 megawatt research reactor, and enable an estimated 2-3 orders of magnitude improvement in sensitivity.

Neutron EDM and lifetime experiments can be pursued using ultra cold neutrons

(UCNs) which have sufficiently low kinetic energy that they can be confined in material or magnetic bottles. However a beam of UCNs does not exist, and the proposed next generation experiments must therefore produce UCNs *in situ* from an incident cold neutron beam. Recently a novel suggestion for the production of UCNs using a spallation target has been undergoing tests at the Los Alamos Neutron Science Center (LANSCE) and elsewhere. The new UCN source concept uses a small target that is very closely coupled to a solid deuterium UCN converter. This makes it possible to significantly increase the density of UCN beyond that obtained using traditional cryogenic moderators, and would therefore be of benefit to the neutron EDM and lifetime experiments which are statistically limited. At the Fermilab Proton Driver one SC linac pulse every few seconds could be used to drive a national UCN facility for neutron EDM and lifetime experiments, and a variety of other scientific programs.

4.2.4 Antiproton Experiments using the MI Beam

The antiproton source at Fermilab is a unique facility. Although built and primarily used to collect antiprotons for the Tevatron Collider, over the years it has also been used to support a more diverse set of experiments which include putting the world's most stringent limits on the antiproton lifetime, studying charmonium states, and providing the first unambiguous observation of atomic antihydrogen. These experiments were performed at the Fermilab Antiproton Accumulator, which provides the world's most intense source of antiprotons. In the Proton Driver era, beyond the period of Tevatron Collider operations, there will exist only one, or possibly two, other antiproton sources in the world - one at GSI, and possibly one at CERN. The Fermilab antiproton source would continue to be the most intense in the world. Indeed, the Fermilab Proton Driver would be expected to enable an increase in the intensity of the present source by about a factor of two. Hence, the Fermilab antiproton source would continue to be a unique facility. The possible antiproton experiments that could be pursued in the future have not been exhaustively studied. However two examples have been considered: The continuation of quarkonium formation studies, and a search for CP violation in hyperon decays.

The study of the charmonium and bottomonium systems has been crucial in unraveling the short-distance properties of the strong interaction. A significant number of important measurements have been made in studies of antiproton-proton formation of charmonium. Note that a gas-jet target experiment in an antiproton storage ring can (i) achieve an energy spread of 10-100 keV (compared with a few MeV in an e^+e^- experiment) allowing precise measurements of heavy- quarkonium masses and widths, and (ii) study the formation of all non-exotic mesons (only 1^{--} states can be directly formed by e^+e^- annihilation). Knowledge of the charmonium and bottomonium spectra is incomplete. There are states to discover, and their masses and widths can help us better understand the strong interaction. For example, in charmonium the h_c must be confirmed, the significant mass discrepancy between the BELLE and BABAR sightings of the η'_c resolved, the h_c and η'_c widths measured, and the other narrow states identified and characterized, namely the $\eta_{c2}(1^1D_2)$, $\psi_2(1^3D_2)[X(3872)?]$, 1^3D_3 , 2^3P_2 , and 1^1F_4 .

There are only a few particle-antiparticle systems that are experimentally accessible and are sensitive to new sources of CP violation. The hyperon-antihyperon system, which can be made in a gas-jet target experiment at the Fermilab antiproton source, is one example. Seeking a deeper understanding of CP violation is important if we are to understand baryogenesis. The Standard Model (SM) predicts a slight *CP* asymmetry in the decays of hyperons [106–112]. Physics beyond the SM can result in large enhancements in this CP asymmetry. For example, the supersymmetric calculation of He *et al.* [113] predicts asymmetries that are up to two orders of magnitude larger than the SM prediction. Although as yet unpublished, the Fermilab HyperCP data is expected to yield measurements of Λ and $\bar{\Lambda}$ decays with sufficient sensitivity to observe CP violation in hyperon decays if it is an order of magnitude larger than the SM prediction. Provided systematic uncertainties can be controlled, an experiment at the Fermilab antiproton source could improve this sensitivity by an order of magnitude, and hence be sufficiently sensitive to observe CP violation at the level predicted by the SM, and precisely measure any enhancement that might be present due to new physics.

5 Compatibilities and Proton Economics

The proton driver design that is currently favored consists of an 8 GeV H^- Linac that initially would produce a 0.5 megawatt beam, and that can eventually be upgraded to produce a 2 megawatt beam. A small fraction of the 8 GeV beam would be used to fill the MI with the maximum beam that, with some modest improvements, it can accelerate. This would yield a 2 megawatt beam at MI energies. Hence the upgraded proton source would deliver two beams that can be simultaneously used for experiments: a 2 megawatt beam at MI energies, and eventually an almost 2 megawatt beam at 8 GeV. To illustrate this the cycle structure is shown in Fig. 15. The MI would receive one pulse from the Linac every 1.5 sec. The cycle time is dominated by the time to ramp up and ramp down the MI energy. The 14 Linac pulses that are available, while the MI is ramping and at flat top, would provide beam for an 8 GeV program.

The initial NUE long-baseline program would be expected to be the primary user of the 2 megawatt MI beam. The high-energy neutrino scattering program also needs this beam, and would be expected to coexist with NUE. The other candidate uses of the MI beam include supporting experiments at an antiproton source, and supporting kaon experiments. The antiproton source could operate in parallel with the MI neutrino program with a modest reduction in the available POT for the NuMI

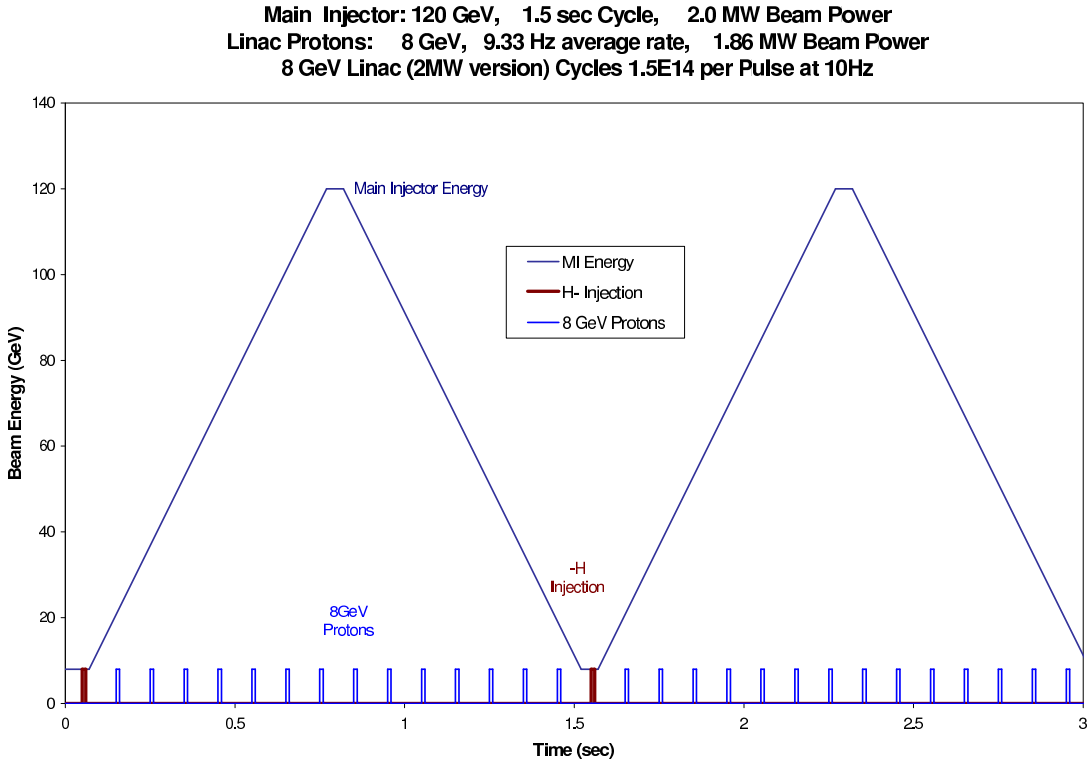


Figure 15: Proton Driver bunch structure and the Main Injector cycle.

beam. The kaon program, in contrast to the neutrino program, would require a slow extracted beam. However, with an additional storage ring, it is possible that a kaon program could be run during neutrino running with only a minor impact on the POT available for the neutrino program. This could be accomplished by fast extraction of a fraction of the MI bunches and transfer into a stretcher ring. The protons stored in the ring would then be slowly extracted for the kaon program. A ring in the Tevatron tunnel would be ideal for this purpose.

The candidates for using the 8 GeV beam are a low energy neutrino scattering experiment, a pion program, a muon program, and a neutron program. The neutrino scattering experiment requires short pulses with large gaps between pulses so that beam-unrelated backgrounds can be suppressed. The pion program requires a beam stretcher to produce long pulses and hence minimize the instantaneous intensity. Many experiments in the muon program require a CW beam with bunches that are short compared to the muon lifetime with gaps between bunches of several muon lifetimes. Hence all of these programs will require an additional storage ring to manipulate the bunch structure. It is possible that, in the post-collider era, this storage ring could be the Recycler. Noting that each of these 8 GeV sub-programs requires a different bunch structure it is natural to consider a scenario in which they run sequentially rather than in parallel. To illustrate this, we can imagine that initially an 8 GeV neutrino scattering experiment is the primary user of the 8 GeV beam, followed by (or possibly interleaved with) one or more pion experiments. In a second phase the facility is upgraded to include a low energy muon source, and one or more low energy muon experiments become the primary user(s). In a third phase, if required, the muon source could be developed to become the front-end of a neutrino factory. This could be a very long-term 20 - 30 year plan.

6 Summary

There is a compelling physics case for a Proton Driver at Fermilab. This upgrade to the existing accelerator complex is motivated by the exciting developments in neutrino physics. Independent of the value of the unknown neutrino mixing parameter θ_{13} , a 2 megawatt Main Injector proton beam would facilitate, over the coming decades, one or more long-baseline neutrino experiments that would make critical contributions to the global neutrino oscillation program. The NuMI beam is the only neutrino beam in the world with an appropriate energy and a long enough baseline for matter effects to significantly change the effective oscillation parameters. With a 2 megawatt Proton Driver this unique feature of the Fermilab neutrino program can be exploited to:

- Probe smaller values of θ_{13} than can be probed with reactor-based experiments or with any existing or approved accelerator-based experiment.
- If θ_{13} is not very small, determine the neutrino mass hierarchy and greatly enhance the sensitivity of the global neutrino program to CP violation.
- If θ_{13} is very small, establish the most stringent limit on θ_{13} and prepare the way for a neutrino factory driven by the Proton Driver.

The MI neutrino oscillation physics program would be supplemented with a broad program of neutrino scattering measurements that are of interest to particle physicists, nuclear physicists, and nuclear astrophysicists. The neutrino scattering program would utilize both the Proton Driver upgraded NuMI beam, and neutrino and anti-neutrino beams generated using the protons available at 8 GeV. The overall neutrino program motivates the highest practical primary beam intensities at both MI energies and at 8 GeV. In practice this means 2 megawatts at MI energies and 0.5-2 megawatts at 8 GeV.

Additional physics programs could also be supported by the Proton Driver. In particular, the Proton Driver could support (i) a program of low energy experiments that probe the TeV mass scale in a way that is complementary to the LHC experiments, and (ii) a program of low energy experiments that are of interest to the nuclear physics community and that is complementary to the JLab program. The possibilities using the 8 GeV beam include (i) the development of a very intense muon source with a bunch structure optimized for (g-2), muon EDM, and LFV muon decay experiments, (ii) a program of low energy pion experiments, and (iii) some specific experiments using spallation neutrons. The possibilities using the MI beam include a program of kaon experiments, and some specific experiments using the antiproton source.

For decades to come, a Fermilab Proton Driver would support an exciting world class neutrino program that would address some of the most fundamental open questions in physics, and could also support a broader program of low energy experiments.

References

- [1] *The Neutrino Matrix* (2004), report from the APS DNP/DPF/DPB Joint Study on the Future of Neutrino Physics.
- [2] T. Yanagida, in *Proceedings of the Workshop on the Unified Theory and the Baryon Number in the Universe*, edited by O. Sawada and A. Sugamoto (KEK, Tsukuba, Japan, 1979), p. 95.
- [3] S. L. Glashow, in *Proceedings of the 1979 Cargèse Summer Institute on Quarks and Leptons*, edited by M. Lévy, J.-L. Basdevant, D. Speiser, J. Weyers, R. Gastmans, and M. Jacob (Plenum Press, New York, 1980), pp. 687–713.
- [4] M. Gell-Mann, P. Ramond, and R. Slansky, in *Supergravity*, edited by P. van Nieuwenhuizen and D. Z. Freedman (North Holland, Amsterdam, 1979), p. 315.
- [5] R. N. Mohapatra and G. Senjanović, Phys. Rev. Lett. **44**, 912 (1980).
- [6] S. Fukuda *et al.* (Super-Kamiokande), Phys. Rev. Lett. **85**, 3999 (2000), hep-ex/0009001.
- [7] Y. Fukuda *et al.* (Super-Kamiokande), Phys. Rev. Lett. **81**, 1562 (1998), hep-ex/9807003.
- [8] K. Lande and P. Wildenhain, Nucl. Phys. Proc. Suppl. **118**, 49 (2003).
- [9] J. N. Abdurashitov *et al.* (SAGE), Phys. Rev. Lett. **83**, 4686 (1999), astro-ph/9907131.
- [10] W. Hampel *et al.* (GALLEX), Phys. Lett. **B447**, 127 (1999).
- [11] Q. R. Ahmad *et al.* (SNO), Phys. Rev. Lett. **87**, 071301 (2001), nucl-ex/0106015.
- [12] S. N. Ahmed *et al.* (SNO), Phys. Rev. Lett. **92**, 181301 (2004), nucl-ex/0309004.
- [13] S. Fukuda *et al.* (Super-Kamiokande), Phys. Lett. **B539**, 179 (2002), hep-ex/0205075.
- [14] M. Apollonio *et al.* (CHOOZ), Phys. Lett. **B466**, 415 (1999), hep-ex/9907037.
- [15] F. Boehm *et al.*, Phys. Rev. **D64**, 112001 (2001), hep-ex/0107009.
- [16] K. Eguchi *et al.* (KamLAND), Phys. Rev. Lett. **90**, 021802 (2003), hep-ex/0212021.
- [17] E. Aliu *et al.* (K2K), Phys. Rev. Lett. **94**, 081802 (2005), hep-ex/0411038.
- [18] A. Aguilar *et al.* (LSND), Phys. Rev. **D64**, 112007 (2001), hep-ex/0104049.
- [19] E. Church *et al.* (BooNe) FERMILAB-PROPOSAL-0898.
- [20] N. Arkani-Hamed, L. J. Hall, H. Murayama, D. R. Smith, and N. Weiner, Phys. Rev. **D64**, 115011 (2001), hep-ph/0006312.
- [21] F. Borzumati and Y. Nomura, Phys. Rev. **D64**, 053005 (2001), hep-ph/0007018.
- [22] R. Kitano, Phys. Lett. **B539**, 102 (2002), hep-ph/0204164.
- [23] R. Arnowitt, B. Dutta, and B. Hu, Nucl. Phys. **B682**, 347 (2004), hep-th/0309033.
- [24] S. Abel, A. Dedes, and K. Tamvakis (2004), hep-ph/0402287.
- [25] H. S. Goh, R. N. Mohapatra, and S.-P. Ng, Phys. Rev. **D68**, 115008 (2003), hep-ph/0308197.
- [26] T. Asaka, W. Buchmüller, and L. Covi, Phys. Lett. **B563**, 209 (2003), hep-ph/0304142.
- [27] K. S. Babu, J. C. Pati, and F. Wilczek, Nucl. Phys. **B566**, 33 (2000), hep-ph/9812538.
- [28] C. H. Albright and S. M. Barr, Phys. Rev. **D64**, 073010 (2001), hep-ph/0104294.
- [29] T. Blazek, S. Raby, and K. Tobe, Phys. Rev. **D62**, 055001 (2000), hep-ph/9912482.
- [30] G. G. Ross and L. Velasco-Sevilla, Nucl. Phys. **B653**, 3 (2003), hep-ph/0208218.
- [31] S. Raby, Phys. Lett. **B561**, 119 (2003), hep-ph/0302027.

- [32] R. Kitano and Y. Mimura, Phys. Rev. **D63**, 016008 (2001), hep-ph/0008269.
- [33] N. Maekawa, Prog. Theor. Phys. **106**, 401 (2001), hep-ph/0104200.
- [34] M.-C. Chen and K. T. Mahanthappa, Phys. Rev. **D68**, 017301 (2003), hep-ph/0212375.
- [35] M. Bando and M. Obara, Prog. Theor. Phys. **109**, 995 (2003), hep-ph/0302034.
- [36] W. Buchmüller and D. Wyler, Phys. Lett. **B521**, 291 (2001), hep-ph/0108216.
- [37] P. H. Frampton and R. N. Mohapatra (2004), hep-ph/0407139.
- [38] W. Grimus and L. Lavoura, JHEP **07**, 045 (2001), hep-ph/0105212.
- [39] W. Grimus and L. Lavoura, Phys. Lett. **B572**, 189 (2003), hep-ph/0305046.
- [40] W. Grimus, A. S. Joshipura, S. Kaneko, L. Lavoura, and M. Tanimoto, JHEP **07**, 078 (2004), hep-ph/0407112.
- [41] S.-L. Chen, M. Frigerio, and E. Ma (2004), hep-ph/0404084.
- [42] I. Aizawa, M. Ishiguro, T. Kitabayashi, and M. Yasue, Phys. Rev. **D70**, 015011 (2004), hep-ph/0405201.
- [43] R. N. Mohapatra, JHEP **10**, 027 (2004), hep-ph/0408187.
- [44] S. Antusch and S. F. King (2004), hep-ph/0402121.
- [45] S. Antusch and S. F. King, Phys. Lett. **B591**, 104 (2004), hep-ph/0403053.
- [46] W. Rodejohann and Z.-z. Xing (2004), hep-ph/0408195.
- [47] K. S. Babu, E. Ma, and J. W. F. Valle, Phys. Lett. **B552**, 207 (2003), hep-ph/0206292.
- [48] T. Ohlsson and G. Seidl, Nucl. Phys. **B643**, 247 (2002), hep-ph/0206087.
- [49] S. F. King and G. G. Ross, Phys. Lett. **B574**, 239 (2003), hep-ph/0307190.
- [50] Q. Shafi and Z. Tavartkiladze, Phys. Lett. **B594**, 177 (2004), hep-ph/0401235.
- [51] M. Bando, S. Kaneko, M. Obara, and M. Tanimoto, Phys. Lett. **B580**, 229 (2004), hep-ph/0309310.
- [52] M. Honda, S. Kaneko, and M. Tanimoto, JHEP **09**, 028 (2003), hep-ph/0303227.
- [53] R. F. Lebed and D. R. Martin, Phys. Rev. **D70**, 013004 (2004), hep-ph/0312219.
- [54] A. Ibarra and G. G. Ross, Phys. Lett. **B575**, 279 (2003), hep-ph/0307051.
- [55] P. F. Harrison and W. G. Scott, Phys. Lett. **B594**, 324 (2004), hep-ph/0403278.
- [56] P. H. Frampton, S. L. Glashow, and T. Yanagida, Phys. Lett. **B548**, 119 (2002), hep-ph/0208157.
- [57] J.-w. Mei and Z.-z. Xing, Phys. Rev. **D69**, 073003 (2004), hep-ph/0312167.
- [58] A. de Gouvea and H. Murayama, Phys. Lett. **B573**, 94 (2003), hep-ph/0301050.
- [59] R. N. Mohapatra, M. K. Parida, and G. Rajasekaran, Phys. Rev. **D69**, 053007 (2004), hep-ph/0301234.
- [60] M.-C. Chen and K. T. Mahanthappa, Int. J. Mod. Phys. **A18**, 5819 (2003), hep-ph/0305088.
- [61] G. Altarelli and F. Feruglio (2004), hep-ph/0405048.
- [62] S. T. Petcov, Phys. Lett. **B110**, 245 (1982).
- [63] C. N. Leung and S. T. Petcov, Phys. Lett. **B125**, 461 (1983).
- [64] M. Fukugita and T. Yanagida, Phys. Lett. **174B**, 45 (1986).

- [65] G. C. Branco, T. Morozumi, B. M. Nobre, and M. N. Rebelo, Nucl. Phys. **B617**, 475 (2001), [hep-ph/0107164](#).
- [66] S. Pascoli, S. T. Petcov, and W. Rodejohann, Phys. Rev. **D68**, 093007 (2003), [hep-ph/0302054](#).
- [67] S. F. King, Phys. Rev. **D67**, 113010 (2003), [hep-ph/0211228](#).
- [68] P. Huber, M. Lindner, M. Rolinec, T. Schwetz, and W. Winter, Phys. Rev. **D70**, 073014 (2004), [hep-ph/0403068](#).
- [69] G. L. Fogli, E. Lisi, A. Marrone, and D. Montanino, Phys. Rev. **D67**, 093006 (2003), [hep-ph/0303064](#).
- [70] M. Maltoni, T. Schwetz, M. A. Tortola, and J. W. F. Valle, Phys. Rev. **D68**, 113010 (2003), [hep-ph/0309130](#).
- [71] Y. f. t. S.-K. C. Hayato, talk given at the HEP2003 conference (Aachen, Germany, 2003), <http://eps2003.physik.rwth-aachen.de>.
- [72] P. Huber, M. Lindner, and W. Winter, Nucl. Phys. **B645**, 3 (2002), [hep-ph/0204352](#).
- [73] M. V. Diwan *et al.*, Phys. Rev. **D68**, 012002 (2003), [hep-ph/0303081](#).
- [74] M. V. Diwan (2004), [hep-ex/0407047](#).
- [75] D. A. Harris *et al.* (Minerva) MINER ν A Note 800, September, 2004, [arXiv:hep-ex/0410010](#).
- [76] L. Auerbach *et al.*, Phys. Rev. D **63**, 112001 (2001), [hep-ex/0101039](#).
- [77] M. Botje, Euro. Phys. Jour. C **14**, 285 (2000).
- [78] X. Ji, Phys. Rev. Lett. p. 610 (1997).
- [79] X. Ji, Phys. Rev. **D55**, 7114 (1997).
- [80] A. Radyushkin, Phys. Lett. **B380**, 417 (1996).
- [81] A. Radyushkin, Phys. Lett. **B385**, 333 (1996).
- [82] J. Collins, L. Frankfurt, and M. Strikman, Phys. Rev. **D56**, 2982 (1997).
- [83] Private communication.
- [84] B. Filippone and X. Ji, Adv. Nucl. Phys. **26**, 1 (2001), [hep-ph/0101224](#).
- [85] S. Bass, R. Crewther, F. Steffens, and A. Thomas, Phys. Rev. **D66**, 031901 (2002).
- [86] M. Jones *et al.*, Phys. Rev. Lett **84**, 1398 (2000).
- [87] O. Gayou *et al.*, Phys. Rev. Lett **88**, 092301 (2002).
- [88] I. Niculescu *et al.*, Phys. Rev. Lett. **85**, 1182 (2000).
- [89] W. Melnitchouk, R. Ent, and C. Keppel Accepted by Physics Reports.
- [90] S. Jeschonnek and J. Van Orden, Phys. Rev. **D69**, 054006 (2004).
- [91] F. Close and N. Isgur, Phys. Lett. **B509**, 81 (2001).
- [92] R. Ent, C. Keppel, and I. Niculescu, Phys. Rev. **D62**, 073008 (2000).
- [93] C. Carlson and N. Mukhopadhyay, Phys. Rev. **D47**, 1737 (1993).
- [94] M. Diemoz, F. Ferroni, and E. Longo, Phys. Rev. **130**, 293 (1986).
- [95] R. Belusevic and D. Rein, Phys. Rev. **D38**, 2753 (1988).
- [96] R. Belusevic and D. Rein, Phys. Rev. **D46**, 3747 (1992).
- [97] R. Shrock, Phys. Rev. **D12**, 2049 (1975).

- [98] A. Amer, Phys. Rev. **D18**, 2290 (1978).
- [99] G. Colangelo and G. Isidori, JHEP **09**, 009 (1998), hep-ph/9808487.
- [100] A. J. Buras and L. Silvestrini, Nucl. Phys. **B546**, 299 (1999), hep-ph/9811471.
- [101] A. J. Buras, G. Colangelo, G. Isidori, A. Romanino, and L. Silvestrini, Nucl. Phys. **B566**, 3 (2000), hep-ph/9908371.
- [102] G. D'Ambrosio, G. F. Giudice, G. Isidori, and A. Strumia, Nucl. Phys. **B645**, 155 (2002), hep-ph/0207036.
- [103] W. J. Marciano and A. Sirlin, Phys. Rev. Lett. **71**, 3629 (1993).
- [104] D. Pocanic *et al.*, Phys. Rev. Lett. **93**, 181803 (2004), hep-ex/0312030.
- [105] Baldo-Ceolin, Z. Phys. **C63**, 409 (1994).
- [106] A. Pais, Phys. Rev. Lett. **3**, 242 (1959).
- [107] Q. Overseth and S. Pakvasa, Phys. Rev. **184**, 1663 (1969).
- [108] J. Donoghue and S. Pakvasa, Phys. Rev. Lett. **55**, 162 (1985).
- [109] J. Donoghue, X. He, and S. Pakvasa, Phys. Rev. **D34**, 833 (1986).
- [110] X. He, H. Steger, and G. Valencia, Phys. Lett. **B272**, 411 (1991).
- [111] G. Valencia Proc. $\bar{p}2000$ Workshop, *op cit.*
- [112] J. Tandean and G. Valencia, Phys. Rev. **D67**, 056001 (2003).
- [113] X. He, H. Murayama, S. Pakvasa, and G. Valencia, Phys. Rev. **D61**, 071701(R) (2000).